Texas Southern University
Digital Scholarship @ Texas Southern University

Dissertations (2016-Present) Dissertations

5-2024

Comparing the Regulatory Effects of Overexpressed MicroRNAs and Xenobiotic Drugs on Cell Cycle and Apoptotic Regulators in PC-3 Cells

Tommie Johnson
Texas Southern University

Follow this and additional works at: https://digitalscholarship.tsu.edu/dissertations

 Part of the Environmental Sciences Commons, Genetics Commons, and the Molecular Biology Commons

Recommended Citation

Johnson, Tommie, "Comparing the Regulatory Effects of Overexpressed MicroRNAs and Xenobiotic Drugs on Cell Cycle and Apoptotic Regulators in PC-3 Cells" (2024). *Dissertations (2016-Present)*. 95.
https://digitalscholarship.tsu.edu/dissertations/95

This Dissertation is brought to you for free and open access by the Dissertations at Digital Scholarship @ Texas Southern University. It has been accepted for inclusion in Dissertations (2016-Present) by an authorized administrator of Digital Scholarship @ Texas Southern University. For more information, please contact haiying.li@tsu.edu.

COMPARING THE REGULATORY EFFECTS OF OVEREXPRESSED MICRORNAS AND XENOBIOTIC DRUGS ON CELL CYCLE AND APOPTOTIC REGULATORS IN PC-3 CELLS

DISSERTATION

Presented in Partial Fulfillment of the Requirements for

the Degree Doctor of Philosophy in the Graduate School

of Texas Southern University

By

Tommie Johnson, B.S., M.S.

Texas Southern University

2024

Approved by

Dr. Shodimu-Emmanuel Olufemi
Chairperson, Dissertation Committee

Dr. Mahesh Vanjani
Dean, The Graduate School

Approved by

Dr. Shodimu-Emmanuel Olufemi	03/28/2024
Chairperson, Dissertation Committee	Date
Dr. Desiree Jackson	03/28/2024
Committee Member	Date
Dr. Hector Miranda	03/28/2024
Committee Member	Date
Dr. Ayodotun Sodipe	03/28/2024
Committee Member	Date
Dr. Bobby Wilson	03/28/2024
Committee Member	Date

© Copyright Tommie Johnson

All Rights Reserved 2024

COMPARING THE REGULATORY EFFECTS OF OVEREXPRESSED MICRORNAS AND XENOBIOTIC DRUGS ON CELL CYCLE AND APOPTOTIC REGULATORS IN PC-3 CELLS

By

Tommie Johnson, Ph.D.

Texas Southern University, 2024

Associate Professor Shodimu-Emmanuel Olufemi, Ph.D., Advisor

MicroRNA was first discovered in C. elegans as small temporal RNA (stRNA) that does not code for protein. Since being discovered they have played a significant role in regulating gene expression at the post-transcriptional level. miRNAs are found in various organisms, and they bind to the 3' untranslated regions to inhibit translation and cause mRNA degradation. Some drugs are involved in cell cycle regulation such as Palbociclib, Ribociclib (LEE011), and Abemaciclib (LY2835219), that causes G1 arrest impeding cell proliferation. Cyclin D1 (CCND1) is supported by the cell cycle making it into a functional product. When undergoing a chemical reaction, the composition of both the cyclins and the cyclin-dependent kinase (CDK), such as CDK4 arrange to replicate the DNA and promote cell division. These drugs could in some cases be involved in regulating the apoptotic pathway since some genes in that pathway are known to influence cell division. Protein Kinase B (AKT) has been known to promote proliferation as well as apoptosis. AKT is key in regulating genes such as B-cell lymphoma extra-large (Bcl-xL), a transmembrane

molecule that prevents the initiation of apoptosis, Caspase-9 (CASP9), that acts as an initiator to cleave other caspases to cause apoptosis to occur. Currently, drugs and microRNAs are used to treat several human diseases. The efficiency between microRNAs and xenobiotic drugs is still in the developing stages and looking at key regulators in both the cell cycle and apoptotic pathway can help draw comparisons between the two in how potent they are. There are two aims for this study. Aim 1: To demonstrate that the overexpression of miRNA (i.e., hsa-miR-3202 and hsa-miR-7152) and xenobiotic drugs (i.e., Abemaciclib ((LY2835219), Ribociclib (LEE011), and Palbociclib) have a similar effect on the cell cycle regulatory gene in PC-3 cells. Aim 2: To demonstrate in PC-3 cells that the overexpression of miRNA (i.e., hsa-miR-3202 and hsa-miR-7152) and xenobiotic drugs (i.e., Abemaciclib ((LY2835219), Ribociclib (LEE011), and Palbociclib) are not similar on the genes in the AKT pathways since the xenobiotic drugs have a direct interaction blockage and the miRNAs affect mRNA translation; even though the miRNAs are not predicted to target the mRNA AKT pathway. We hypothesize that overexpression of the miRNAs or the xenobiotic drugs in PC-3 cells will similarly reduce the protein expression of CDK4, CDK6, and cyclin D1 since the miRNAs have a higher target predicted score at the miRDB (miR DataBase). As well as overexpression of miRNAs (i.e., hsa-miR-3202 and hsa-miR-7152) will reduce protein expression of genes in the AKT pathways but the xenobiotic drugs (i.e., Abemaciclib ((LY2835219), Ribociclib (LEE011), and Palbociclib) will not. The results suggested that the xenobiotic drugs ultimately inhibit the protein expression of the cell cycle and apoptotic regulators in PC-3 cells as compared to the overexpressed microRNAs. This is the first report that compared and showed that

overexpressed miRs are less potent than xenobiotic drugs that directly interact with their target proteins. The result suggests that miRNA tested in the study as compared to the drugs may be less harmful or toxic to cells. Yet other miRNAs may be more potent, especially those miRNAs that function as tumor suppressors or oncogenes. The results also show that genes in the AKT pathway, which is upstream of our target genes, are also affected by the miRNA and the xenobiotic drugs to a certain extent in PC-3 cells.

TABLE OF CONTENTS

LIST OF FIGURES

Figures Page

LIST OF TABLES

Tables Page

LIST OF ABBREVIATIONS

1C8	Non-Invasive Melanoma Cell
3' UTR	3' untranslated region
A1	Alpha-1
Apaf-1	Apoptosis-Activating Factor 1
ACTIN	Beta-Actin
AGO	Argonaute
AKT	Protein Kinase B
AKT1	PKB-α
AKT2	PKB-β
AKT3	PKB-γ
AR	Androgen Receptor
BAD	Bcl-2-associated death promoter
BAK	Bcl-2 homologous antagonist/killer
BAX	Bcl-2-like protein 4
Bcl-2	B-cell lymphoma 2
Bcl-xL	B-cell lymphoma-extra large
Bcl-w	Bcl-2-like protein 2
Bf-l	Bcl-2-related protein A1
BID	BH3 interacting-domain death agonist
BIK	Bcl-2-interacting killer
BIM	Bcl-2-like protein 11

BMF	Bcl2 modifying factor
CARD	Caspase Activation Domain
CASP9	Caspase 9
CBC	Complete Blood Count
CCND1	Cyclin D1
CCND3	Cyclin D3
CDK4	Cyclin-Dependent Kinase 4
CDK6	Cyclin-Dependent Kinase 6
CKIs	Cyclin Kinase Inhibitors
C. elegans	*Caenorhabditis elegans*
DGCR8	DiGeorge syndrome critical region gene 8
DNMT1	DNA methyltransferase 1
dsRNA	Double-Stranded RNA
Erα	Estrogen Receptor Alpha
Exp-5	Exportin 5
FFPE	Formalin-Fixed Paraffin-Embedded
FOXM1	Forkhead Box M1
GSK3β	Glycogen Synthase Kinase 3β
HAT	Histone Acetyltransferase
HCC	Hepatocellular Carcinoma
HDAC	Histone Deacetylases
HMGA2	High Mobility Group AT-Hook 2
HRK	Harakiri

Hsp90	Heat shock protein 90
Ki	Inhibitor constant
L1	Larval Stage 1
L2	Larval Stage 2
LEE011	Ribociclib
LPH	Liposome-polycation-hyaluronic acid
LY2835219	Abemaciclib
M2	N-desethylabemaciclib
M18	hydroxy-N-desethylabemaciclib
M20	hydroxyabemaciclib
Mcl-1	Myeloid cell leukemia 1
miRNAs	microRNAs
mRNA	messenger RNA
miRNP	microRNA ribonucleoprotein complex
MRT	Malignant Rhabdoid Tumor
NOXA	Phorbol-12-myristate-13-acetate-induced protein 1
P/CAF	P300/CBP-Associated Factor
PD-0332991	Palbociclib
PDCD4	Programmed Cell Death 4
PFS	Progression-Free Survival
PH	Pleckstrin Homology
PI3K	Phosphatidylinositol 3-kinase
pre-miRNA	Precursor miRNA
PTEN	Phosphatase and Tensin Homolog

PUMA	p53 upregulated modulator of apoptosis
qRT-PCR	Quantitative Real-Time PCR
Rb	Retinoblastoma Protein
RISC	RNA-induced silencing complex
ROS	Reactive Oxygen Species
RTK	Receptor tyrosine kinase
SD	Stable Disease
shRNAs	Endogenous Short Hairpin RNAs
snoRNAs	Small Nucleolar RNAs
T1C3	Invasive Melanoma Cell
TGF-β	Transforming Growth Factor Beta
TNRC6A	Trinucleotide Repeat-Containing Gene 6A
TPM1	Tropomyosin 1

VITA

December 2013.....	B.S., Texas Southern University Houston, Texas
May 2016.....	M.Sc. Texas Southern University Houston, Texas
2014-2024……..….....	Graduate Teaching Assistant Department of Biology College of Science, Engineering & Technology Texas Southern University Houston, Texas
2018-2021.....	Graduate Research Assistant Department of Environmental & Interdisciplinary Science (EIS), College. Of Science, Engineering &Technology Texas Southern University Houston, Texas
Major Field.....	Environmental Toxicology

ACKNOWLEDGEMENTS

I would like to thank God for all his blessing. I would like to express my appreciation and upmost respect to my advisor, Dr. Shodimu-Emmanuel Olufemi. His proficiency, honesty, and patience added considerably to my graduate research experiences. His encouragement, and immense wisdom which were the important aspects throughout my Master's. Dr. Olufemi has been my advisor and mentor, giving me guidance and encouragement throughout my matriculation at Texas Southern University. I am truly thankful for his unwavering integrity and selfless dedication to both my personal and academic development. I cannot think of a better advisor to have. He is a mentor and father figure. I have obtained the vital skill of discipline, critical thinking. His overseeing of my technical writing has been a blessing. He has always found the time to propose consistently excellent improvements. To him I owe a great debt of gratitude to Dr. Olufemi.

I would also like to thank my committee members Dr. Desirée Jackson, Dr. Hector C. Miranda Jr., and Dr. Bobby Wilson. I thank them for their kind effort and support in the completion of this thesis, and their excellent feedback on an earlier version of this thesis.

I would also like to thank my family for the kind support they provided me through my entire life, and I must acknowledge my mother and father, Tamitra Mosley and Louis Mosley, without their love, advice, and encouragement, I would not have finished this thesis. I would like to thank my brothers and sisters for believing in me and for their continuous encouragement, without their constant motivation I could not have gotten this far. I would like to thank the best lab mates Dr. Hoda Eltayeb "princess", Dr. Mounira Morgem and the rest of "TEAM EMPIRE." I would like to thank my awesome friend Dr.

Samrawit Yeshitla, for her bonding support and snacks helped with me spending more hours in the lab and for being a great friend.

I would like to thank the special administrative assistant Ms. Rachel Mizzell in the Department of Environmental Toxicology for her continuous support, availability, and proficiency in helping me and most importantly with ordering materials. I thank Mrs. Helen Pittman-Cockrell for her guidance, kindness, and encouragement during my years as a graduate student at Texas Southern University; and with always working with my schedule while assigning classes as a Graduate Teaching Assistant in the Department of Biology.

CHAPTER 1

INTRODUCTION

Lee and colleagues made a groundbreaking discovery regarding microRNAs (miRNAs) in the nematode Caenorhabditis elegans (*C. elegans*) (Lee et al., 1993). MiRNAs are a class of small, conserved RNA molecules that play a crucial role in posttranscriptional gene expression regulation. Ranging from 19 to 24 nucleotides in length, they function by binding to target sequences on messenger RNA (mRNA) molecules, thereby inhibiting or redirecting the translation process and affecting protein production (Lee et al., 1993). MicroRNA genes exhibit considerable variation in their genomic locations. Previous investigations have identified two distinct classes of miRNAs: those originating from overlapping introns of protein-coding transcripts and others encoded within exons. These findings underscore the intricate nature of miRNA maturation processes (Rodriguez et al., 2004). Additionally, researchers have uncovered clusters of miRNA genes that are co-expressed as polycistronic units, indicating the potential for transcription as a single entity (Lagos et al., 2003; Lau et al., 2001). Approximately 50% of miRNAs are estimated to be expressed from non-protein coding transcripts, while the remaining majority is primarily located in coding gene introns and usually transcribed together with their host genes but processed separately (Saini et al., 2007).

As this field is rapidly advancing, future developments have the potential to revolutionize our current understanding of miRNA genesis. Based on existing knowledge, it can be concluded that genomic regions capable of generating mature and functional

miRNAs can be found in various locations throughout the genome. Breast cancer took the spotlight early on in microRNA research, especially in 2005. Iorio and colleagues made a groundbreaking discovery by unveiling the first distinct microRNA signature exclusive to breast carcinoma. Their meticulous investigation pinpointed 13 microRNAs with an astonishing 100% accuracy in distinguishing between tumor and normal tissues (Iorio et. al., 2005) These special microRNAs that exhibited differential expression became the subject of extensive scrutiny due to their pivotal role in breast cancer biology. Some drugs are known to play an important role in treating breast cancer. They are Abemaciclib ((LY2835219), Ribociclib (LEE001) and Palbociclib which functions in inhibiting the main cell cycle regulators of Cyclin D1 (CCND1), a key player in regulating the progression of the cell cycle within the nucleus (Kato et al., 1993), Cyclin-Dependent Kinase 4 (CDK4) and Cyclin-Dependent Kinase 6 (CDK6), both of whose primary function is to facilitate the progression from G1 to S phase by phosphorylating and deactivating the retinoblastoma protein (RB) (Vora et al., 2014).

The overexpression of these cell cycle regulators can lead to overproduction of many cancer cell types. There is also another mechanism known as apoptosis, which is promoted upstream by protein kinase B (AKT), that acts on a proapoptotic gene B-cell lymphoma-extra-large (Bcl-xL) to promote proliferation and the gene that initiates apoptosis Caspase 9 (CASP9), which activates the gene Caspase 3 (CASP3) to promote cell death (Manning and Toker, 2017; Mundi et al., 2016; Tsujimoto and Croce, 1986; Bratton and Salvesen 2010; Li et al., 1997).

Based on the miR database and journals discussing the half concentration dosage of the xenobiotic drugs, we hypothesize that both the overexpressed microRNAs and the

xenobiotic drugs will show the same efficiency and will reduce expression of the cell cycle regulators, CCND1 and CDK4 as well the apoptotic regulators AKT, Bcl-xL and CASP9. These key regulators were selected for the initial study. To achieve the objective of this study, miRNAs that target the mRNA of CDK4, CDK6, and cyclin D1, including the xenobiotic drugs, would be used individually to treat PC-3 cells. Western blot would detect differences in the protein expression between the overexpressed miRNAs and the xenobiotic drugs.

The genes of interest are the cell cycle and anti/pro-apoptotic regulator genes, such as CCND1, CDK4, AKT, Bcl-xL, and CASP9. The experiment will establish if overexpression of miRNAs is suitable and potent or toxic in regulating cell proliferation in cancer cells. There are two aims for this study. Aim 1: To demonstrate that the overexpression of miRNA (i.e., hsa-miR-3202 and hsa-miR-7152) and xenobiotic drugs (i.e., Abemaciclib ((LY2835219), Ribociclib (LEE011), and Palbociclib) have a similar effect on the cell cycle regulatory gene in PC-3 cells. Aim 2: To demonstrate in PC-3 cells that the overexpression of miRNA (i.e., hsa-miR-3202 and hsa-miR-7152) and xenobiotic drugs (i.e., Abemaciclib ((LY2835219), Ribociclib (LEE011), and Palbociclib) are not similar on the genes in the AKT pathways since the xenobiotic drugs have a direct interaction blockage and the miRNAs affect mRNA translation; even though the miRNAs are not predicted to target the mRNA AKT pathway. We hypothesize that overexpression of the miRNAs or the xenobiotic drugs in PC-3 cells will similarly reduce the protein expression of CDK4 and cyclin D1 since the miRNAs have a higher target predicted score at the miRDB (miR DataBase). As well as the overexpression of miRNAs (i.e., hsa-miR-3202 and hsa-miR-7152) will reduce protein expression of genes in the AKT pathways but

the xenobiotic drugs (i.e., Abemaciclib ((LY2835219), Ribociclib (LEE011), and Palbociclib) will not. The results suggested that the xenobiotic drugs ultimately inhibit the protein expression of the cell cycle and apoptotic regulators in PC-3 cells as compared to the overexpressed microRNAs. This is the first report that compared and showed that overexpression miRs are less potent than xenobiotic drugs that directly interact with their target proteins. The result suggests that miRNA tested in the study as compared to the drugs may be less harmful or toxic to cells. Yet other miRNAs may be more potent, especially those miRNAs that function as tumor suppressors or oncogenes. The results also show that genes in the AKT pathway, which is upstream of our target genes, are also affected by the miRNA and the xenobiotic drugs to a certain extent in PC-3 cells.

CHAPTER 2

LITERARY REVIEW

microRNAs (miRNAs)

Further investigations have revealed that miRNAs not only suppress translation but also interact with mRNA decay factors when bound to their target mRNA, leading to destabilization, degradation, and reduction in gene expression levels. The downregulation of the LIN-14 gene in *C. elegans* is crucial for the transition from the first larval stage (L1) to L2. Interestingly, this downregulation is dependent on the presence of another transcribed gene called lin-4, which does not produce an active protein during translation. Instead, it generates two small RNAs approximately 21 to 61 nucleotides long. The longer RNA forms a stem-loop structure and serves as a precursor for the shorter RNA (Lee et al., 1993), along with Wightman et al. (1993), later discovered that the shorter RNA exhibits antisense complementarity to multiple sites in the 3' untranslated region (3' UTR) of lin-14 mRNA. The complementary interaction between these regions leads to reduced expression of the LIN-14 protein without significantly altering mRNA levels. These two studies provided strong evidence supporting the notion that repression of lin-14 translation and progression from L1 to L2 stages during C. elegans development is facilitated by the base pairing of multiple lin-4 small RNAs with complementary sites in the lin-14 mRNA 3' UTR.

The transcription of miRNA coding transcripts initially occurs through RNA polymerase II, generating long primary transcripts that contain a 5' guanosine cap and a 3'

polyadenylated tail. These primary transcripts can be either non-coding or coding in nature. Subsequently, a multiprotein complex called the Microprocessor processes the primary miRNA into precursor RNA (pre-miRNA), which typically ranges from around 70 to 120 nucleotides in length. The Microprocessor complex includes Drosha, a highly conserved ~160-kDa nuclear RNase III enzyme found in animals (Lee et al., 2003). However, Drosha is not conserved in plants (Wu et al., 2000). Drosha forms a dimer with another double-stranded RNA (dsRNA) binding protein called DiGeorge syndrome critical region gene 8 (DGCR8) or Pasha, creating a functional Microprocessor complex (Denli et al., 2004; Gregory et al., 2004; Han et al., 2004; and Landthaler et al., 2004). The newly formed pre-miRNA, characterized by a typical 5' phosphate and a ~2-nucleotide 3' overhang, is subsequently exported to the cytoplasm by exportin 5 (Exp-5), a Ran-dependent nuclear transport receptor protein (Lund et al., 2004; Yi et al., 2003). In the cytoplasm, pre-miRNAs undergo their final processing into mature duplexes approximately 18 to 23 nucleotides in length. This processing is facilitated by another RNase III enzyme called Dicer-1, in conjunction with dsRNA-binding proteins such as protein kinase RNA activator and transactivation response RNA binding protein (Chendrimada et al., 2005; Lee et al., 2006; Lee et al., 2002; Yi et al., 2003).

The resulting miRNA duplexes are then separated based on factors like thermodynamic asymmetry and stability of base pairing at the 5' end. Typically, the strand with the least stable base pairing at the 5' end becomes the guide strand, which, along with RNA binding proteins including trinucleotide repeat-containing gene 6A (TNRC6A), associates with Argonaute (AGO) proteins, forming a microRNA ribonucleoprotein complex (miRNP) called the RNA-induced silencing complex (RISC) (Schwarz et al.,

2003). The strand with stable base pairing at the 5' end is often degraded or, in rare cases, can also associate with AGO proteins, enabling both strands to function as miRNAs (Czech et al., 2009; Okamura et al., 2009). The guide strand directs the RISC complex to the target mRNA through sequence complementarity, leading to translational repression. AGO proteins, particularly Ago2, have been localized to cytoplasmic structures known as GW/P-bodies, where miRNAs bound to their mRNA targets are stored for degradation or translational repression (Castilla-Llorente et al., 2012). Nevertheless, emerging evidence suggests that miRNA biogenesis can occur independently of the Microprocessor complex. Examples include pre-miRNA-like hairpins called "Mirtrons," which arise from spliced and debranched short hairpin introns, as well as small nucleolar RNAs (snoRNAs) and endogenous short hairpin RNAs (shRNAs) (Babiarz et al., 2008; Ender et al., 2008; Okamura et al., 2007; Saraiya and Wang, 2008).

Notably, miR-21 plays a crucial role in showing heightened expression in breast carcinoma. It proved to be a significant regulator of cell survival and proliferation, directly targeting tumor suppressor genes PTEN (Phosphatase and Tensin Homolog), PDCD4 (Programmed Cell Death 4), and TPM1 (Tropomyosin 1). Its overexpression also correlated with advanced clinical stages, lymph node metastasis, and patients' poor prognosis (Yan et al., 2008; Qian et al., 2009). Interestingly, miR-21's impact extended beyond breast cancer, as it is overexpressed in other malignancies, including glioblastoma, ovarian cancer, and lung cancer (Chan et al., 2005; Ciafre et al., 2005; Iorio et al., 2007; Yanaihara et al., 2006; Markou et al., 2008; and Volinia et al., 2006). Another microRNA of great significance is let-7, initially discovered as a tumor suppressor in the tiny worm C. elegans. Interestingly, let 7 is known to be a novel regulator influencing self-renewal and

tumorigenicity in breast cancer cells. By targeting molecules previously associated with lung cancer, such as RAS29, HMGA2 oncogene HMGA2 (High Mobility Group AT-Hook 2), and even MYC, let-7 displays its multifaceted role (Johnson et al., 2005; Mayr et al., 2007; and Sampson et al., 2007).

In mouse models dealing with breast and lung cancer, the overexpression of let-7 microRNA family members has shown promising tumor-suppressive effects (Yu et al., 2007; Kumar et al., 2008). Moving to hepatocellular carcinoma (HCC), Murakami and colleagues (2006) reported that miR-222, miR-106a, and the miR-17-92 cluster are involved with tumor differentiation levels. Conversely, higher levels of the oncosuppressor miR-125b are associated with improved survival rates (Li et al., 2008). MiR-125b has also exhibited growth inhibition properties in vitro, as demonstrated in a human thyroid anaplastic carcinoma model (Visone et al., 2007).

The effective delivery of gene-based therapy remains a significant challenge, primarily concerning the precise targeting of therapeutics while avoiding degradation or undesired elimination. MicroRNAs offer clear advantages due to their small size and water solubility, enabling intravascular or subcutaneous administration. However, once inside the body, miRNAs face rapid degradation and widespread excretion through the kidneys (Trang et al., 2011). Consequently, researchers are actively investigating strategies to target miRNA mimics or inhibitors to specific tissues or cell types. Delivery of miRNAs using nanoparticles larger than 100 nm often leads to accumulation in the liver, spleen, lung, and bone marrow, with non-specific uptake and subsequent excretion (Longmire et al., 2008). Also, systemic administration of miRNAs in cationic liposomes can induce toxicity through toll-like receptor-mediated and immune responses (Lv et al., 2006). To overcome

these challenges, some studies have utilized the inherent properties of delivery vectors to direct miRNA delivery to specific organs, while others have incorporated targeting antibodies on vectors for cell-type-specific uptake (Chen et al., 2010). Local delivery of nucleic acids generally presents a lower risk of side effects than systemic delivery, although not all target tissues are suitable for this approach. Systemic delivery methods are more complex, involving the vector and miRNA traversing the bloodstream to reach the intended destination. Viral vectors currently exhibit the highest efficacy for miRNA delivery into cells, but their safety remains a subject of controversy. Lipid delivery vectors, with miRNA protected inside lipid bilayers, offer attractive features by delivering their contents directly into cells, bypassing endosome and lysosome degradation. The field of nanoparticle and polymer delivery systems for gene therapy continues to expand, employing various vectors for in vivo miRNA delivery, such as modified PEG, inorganic nanoparticles, and targeted nanoparticles. For instance, a Liposome-polycation-hyaluronic acid (LPH)-PEG-GC4 particle containing a mimic miR-34a reduced lung tumor burden in a mouse model with melanoma metastasis (Chen et al., 2010).

Abemaciclib (LY2835219)

Abemaciclib, also known as (LY2835219), is a highly selective and potent oral inhibitor that targets Cyclin-Dependent Kinase 4 (CDK4) and Cyclin-Dependent Kinase 6 (CDK6). By blocking CDK4 and CDK6, abemaciclib induces G1 arrest and impedes cell proliferation. It achieves this by causing the dephosphorylation of the retinoblastoma tumor suppressor protein (Dickler et al., 2016; Patnaik et al., 2016; Gelbert et al., 2014). Unlike other CDK4 and CDK6 inhibitors such as Ribociclib and Palbociclib, Abemaciclib exhibits a distinct molecular structure and demonstrates 14 times higher effectiveness in enzymatic

assays against Cyclin D1 (CCND1)/CDK6 and Cyclin D3 (CCND3)/CDK6 (Patnaik et al., 2016; Gelbert et al., 2014; Lallena et al., 2015; Pfizer; Novartis Pharmaceuticals). Extensive pre-clinical studies have revealed the multifaceted actions of Abemaciclib in tumor cells. It has demonstrated synergy with immune checkpoint therapy by stimulating anti-tumor immune responses and modifying tumor metabolic activities (Ameratunga et al., 2019; Klein et al., 2018).

Abemaciclib undergoes metabolic processes resulting in the production of several metabolites; however, the primary components found in plasma exposure are abemaciclib itself, hydroxyabemaciclib (M20), N-desethylabemaciclib (M2), and hydroxy-N-desethylabemaciclib (M18) (Verzenio 2018). Abemaciclib exhibits selective inhibition of CDK4/6, with a Ki (inhibitor constant) value of 0.6 nM for cyclin D1/CDK4 and 8.2 nM for cyclin D3/CDK6 (Burke et al., 2016). The metabolites M2, M18, and M20 display IC50 values between 1 and 3 nm for inhibiting CDK4 and CDK6, which are comparable in potency to Abemaciclib (Tripathy et al., 2017). In both in vitro and in vivo environments, Abemaciclib has demonstrated remarkable efficacy in suppressing Rb phosphorylation and inducing cell cycle arrest in the G1 phase. In various tumor xenograft growth models, including breast cancer, Abemaciclib effectively inhibits cancer cell growth by competitively binding to the ATP sites within the catalytic region of CDKs, thereby preventing ATP binding (Sánchez-Martínez et al., 2015).

Ribociclib (LEE001)

Ribociclib, also known as LEE011, is a small selective molecule that effectively blocks the phosphorylation of the retinoblastoma protein, thereby halting the progression of the cell cycle and inducing G1 phase arrest by inhibiting the expression of CDK4/6 (Kim

et al., 2013). Ribociclib exhibits high selectivity and possesses large binding-site side chains, reducing the likelihood of interactions with off-target kinase ATP-binding pockets due to its significant lipophilicity (Chen et al., 2016). In studies involving estrogen receptor-positive breast cancer xenograft models, Ribociclib demonstrated antitumor activity when administered alone or in combination with letrozole and phosphatidylinositol 3-kinase (PI3K) inhibitors (O'Brien et al., 2014). Initially investigated in patients with lymphomas and advanced solid tumors, Ribociclib was directly involved in a phase I study of 132 patients, with 125 patients following a 21-day on, 7-day off schedule, and seven patients receiving continuous dosing. Of the participants, three patients showed partial response (PR), and 43 patients achieved the best results to the stable disease (SD). Notably, eight patients with various tumor types, such as squamous cell carcinomas of the head and neck, teratomas, and liposarcomas, experienced progression-free survival (PFS) for over six months (Infante et al., 2016).

While breast cancer has been the primary focus of Ribociclib research, it is also being experimented in other malignancies. For instance, investigations are underway to evaluate its efficacy in pediatric neuroblastoma and malignant rhabdoid tumor (MRT). In a study involving 32 pediatric patients aged 1 to 21 years, different doses of Ribociclib were given, and three patients experienced dose-limiting fatigue or thrombocytopenia. Moreover, seven neuroblastoma patients and two patients with primary CNS MRT achieved stable disease between 6 to 13 cycles of Ribociclib (Geoerger et al., 2017). Common adverse effects associated with Ribociclib are similar to those observed with palbociclib and include neutropenia, leukopenia, fatigue, and nausea (Infante et al., 2016; Bardia et al., 2014; Munster et al., 2017; Tolaney et al., 2016; and Bardia et al., 2015).

Neutropenia induced by Ribociclib is administered through regular complete blood count (CBC) monitoring, appropriate treatment of accompanying fevers or infections, and potential dose reduction or treatment interruption depending on the severity (Spring et al., 2017). Notably, Ribociclib-induced neutropenia tends to be more rapidly reversible compared to neutropenia associated with cytotoxic chemotherapy, which is why Ribociclib is administered in a standard 21-day on and 7-day off regimen (Asghar et al., 2015). The acceptable safety profile of Ribociclib supports its continued investigation (Infante et al., 2016).

Palbociclib

Palbociclib, also referred to as PD-0332991, is an orally administered drug that exhibits high selectivity in targeting cyclin-dependent kinase 4 (CDK4) and cyclin-dependent kinase 6 (CDK6). By inhibiting these enzymes, palbociclib disrupts the phosphorylation of retinoblastoma protein (Rb), leading to cell cycle arrest at the G1 phase. This mechanism effectively hinders the proliferation of tumor cells by downregulating the expression of the transcription factor E2F, which governs genes involved in cell cycle progression (Fry et al., 2004; Toogood et al., 2005). Preclinical investigations have demonstrated the impressive efficacy of palbociclib, particularly in primary bone marrow myeloma cells and xenograft models, where it exhibits significant tumor growth inhibition. Furthermore, combining palbociclib with other agents has shown enhanced potency (Baughn et al., 2006).

In clinical practice, palbociclib has gained FDA approval for the treatment of metastatic hormone receptor-positive, HER2-negative breast cancer in combination with letrozole, based on favorable outcomes from trials like PALOMA-1 and PALOMA-2.

Ongoing research is actively exploring the potential of palbociclib in other hematologic malignancies, such as mantle cell lymphoma, where it has displayed promise in suppressing cancer cell growth. With its manageable safety profile and ongoing research efforts, palbociclib holds great potential as a therapeutic option across various cancer types (Finn et al., 2015; Finn et al., 2016; Beaver et al., 2015; Marzec et al., 2006; Leonard et al., 2012).

Cyclin D1 (CCND1)

Cyclin D1's main job is to facilitate the transition from the G1 phase to the S phase by acting as a regulator for cyclin-dependent kinase 4 (CDK4) and CDK6. Cyclin D1 and CDK4 form an active complex that moves into the nucleus. They combine with Cyclin E/CDK2 to phosphorylate the retinoblastoma (RB) protein. This phosphorylation event, along with the relaxation of control on the E2F transcription factor, paves the way for the activation of specific genes that play a crucial role in cell growth and division (Kato et al., 1993; Lundberg et al., 1998). Excessive production of Cyclin D1 triggers uncontrolled growth of cells, which in turn promotes the development of tumors. This highlights the significant role Cyclin D1 plays in the onset and progression of cancer. Cyclin D1 is encoded by the CCND1 gene found on chromosome 11q13 and has a size of 36-kDa protein. While it is typically expressed in most normal human cells, cells derived from bone marrow stem cell lines do not display Cyclin D1 expression (Inaba et al., 1992). The structure of Cyclin D1 consists of various functional domains, including a region that binds to the RB protein that interacts with cyclin-dependent kinases (CDKs) or CDK inhibitors, an LxxLL motif responsible for recruiting coactivators, a PEST site that governs the degradation of Cyclin D1, and a residual threonine that regulates the export of the protein

from the nucleus as well as its stability (Musgrove et al., 2011). Cyclin D1 is crucial in cell cycle regulation through its interactions with CDK-dependent mechanisms. It kickstarts the process by initiating RB phosphorylation, which is significant in controlling cell growth and division.

Moreover, Cyclin D1 facilitates by making sure that other proteins can perform their jobs effectively by adjusting the binding of histone deacetylases (HDAC). Apart from these CDK-dependent functions, Cyclin D1's role as a gene expression manager influences the activity of different transcription factors that oversee the cell cycle. For instance, it puts the brakes on mediators of transforming growth factor beta (TGF-β), like Smad3, allowing the cell to progress beyond the G1 phase and move forward (Zelivianski et al., 2010). Additionally, Cyclin D1 activates the transcriptional function of an essential regulator called forkhead Box M1 (FOXM1), which controls several factors involving the transitioning from the G1 phase to the S phase. Activation of Cyclin D1 in cancer cells leaves a profound impact. It leads to a decrease in reactive oxygen species (ROS) and halts cellular senescence, ultimately supporting the survival and rapid growth of these cells (Anders et al., 2011). Cyclin D1 also forms associations with specific protein complexes, such as histone acetyltransferase (HAT) complexes like P300/CBP-associated factor (P/CAF), allowing Cyclin D1 to regulate the activity of estrogen receptor alpha (ERα) and androgen receptor (AR) in breast and prostate epithelial cells (McMahon et al., 1999; Reutens et al., 2001). These discoveries open new possibilities and shed light on the potential connections between Cyclin D1 and cellular metabolism. Ultimately, they influence the pace at which cancer cells grow and proliferate.

Cyclin-Dependent Kinase 4 (CDK4)

CDKs are complex enzymes composed of two components: a regulatory subunit called cyclin and a catalytic subunit known as cyclin-dependent kinase (Malumbres and Barbacid 2009; Morgan 1997; and Malumbres and Barbacid 2001). These serine/threonine kinases have approximately 300 amino acids in their catalytic domains and remain inactive when they are underphosphorylated and exist as individual units (Morgan 1997). The primary mechanism of CDK activation involves binding to specific regulatory cyclins. Unlike CDKs, cyclins are a diverse family of proteins with sizes ranging from approximately 35 to 90 kDa (Malumbres and Barbacid, 2009; Morgan, 1997; Graña and Reddy, 1995). In the case of CDK4, phosphorylation occurs at Thr172 (Kato et al., 1994). Notably, the activity of this protein complex remains constant regardless of the cell cycle phase and is even present in quiescent cells (Larochelle et al., 1998). CDK4/6 complexes associate with D-type cyclins and facilitate progression through the G1 phase, a preparatory phase for DNA synthesis. The activation of CDK4/6/CYCLIN D complexes contributes to the hyperphosphorylation of the retinoblastoma (RB) protein and its related proteins, p107 and p130. The non-phosphorylated form of pRB binds to and sequesters several cellular proteins, while its phosphorylation leads to the release of these protein factors. The CDK subunit can be phosphorylated by regulatory kinases at inhibitory sites near the N-terminus. The activity of CYCLIN/CDK complexes can also be controlled negatively in a tissue-specific manner by two families of cyclin kinase inhibitors (CKIs): the INK4 and CIP/KIP families of proteins (Malumbres and Barbacid, 2009; Gil and Peters, 2006; Blain, 2008; Denicourt and Dowdy, 2004; Cánepa et al., 2007; Li et al., 2011).

The group of proteins called INK4, which includes p16INK4A, p15INK4B, p18INK4C, and p19INK4D, hinders the activity of CDK4 and CDK6 by forming specific associations with them. These inhibitory proteins are expressed at minimal levels or remain undetectable in actively dividing cells. However, signals induce them to inhibit cell growth, such as contact inhibition, senescence, or exposure to certain growth-inhibiting factors (Blain 2008). Interestingly, the protein p27 is present throughout the cell cycle, and a significant proportion of it in dividing cells is known to bind to CYCLIN D-CDK4 complexes. Remarkably, these p27-CYCLIN D-CDK4 complexes retain kinase activity, suggesting that their interaction does not lead to CDK4 inhibition (Blain et al., 1997; Soos et al., 1996; Mahony et al., 1998; James et al., 2008; Sugimoto et al., 2002; Bagui et al., 2003; Toyoshima et al., 1994; Polyalk et al., 1994; Larrea et al., 2008; Blain, 2008; and Denicourt and Dowdy, 2004). One extensively studied target of G1 CYCLIN/CDK complexes is the protein RB, which undergoes phosphorylation in a cell cycle-dependent manner. RB exhibits minimal phosphorylation in non-dividing cells but becomes phosphorylated at specific sites (Ser780 and Ser795) by CDK4/CDK6 during the later stages of the G1 phase. The unphosphorylated form of RB interacts with various cellular proteins, and its phosphorylation results in the dissociation of RB from its binding partners (Kitagawa et al., 1996; Connell-Crowley et al., 1997; Grafstrom et al., 1999). Insights from the crystal structures of CDK4/Cyclin D complexes suggest that the active conformation of CDK4 relies heavily on its binding to both substrate and cyclin (Takaki et al., 2009).

Protein Kinase B (PKB & AKT)

AKT, a serine-threonine kinase, plays a critical role in numerous biological processes that include cell proliferation, survival, glucose metabolism, protein synthesis,

genome stability, and the prevention of apoptosis in response to various growth factors and external stimuli (Manning and Toker, 2017; Mundi et al., 2016). Its activation has been observed in multiple types of human cancer, contributing to tumor aggressiveness and resistance to drugs in many cases (Cheon et al., 2011; Singh and Johnson, 2006). AKT regulates several pathways associated with cancer-related characteristics. It inhibits pro-apoptotic proteins such as BCL-2-antagonist of cell death (BAD) and procaspase-9 to impede apoptosis. Additionally, AKT phosphorylates and inhibits glycogen synthase kinase 3β (GSK3β) to prevent the degradation of cyclin D1 during cell cycle progression (Arcaro and Guerreiro, 2007; Downard, 2004; and Testa and Bellacosa, 2001). There are three isoforms of AKT (AKT1/PKB-α, AKT2/PKB-β, and AKT3/PKB-γ) present in humans sharing common structures and similar activation mechanisms (Wang et al., 2018). The N-terminus of AKT features a pleckstrin homology (PH) domain that interacts with membrane lipids, facilitating the recognition of AKT and its translocation to the membrane by upstream kinases (Hanada et al., 2004). The central catalytic region of the protein contains the kinase domain, housing a threonine residue that necessitates phosphorylation for AKT activation (Hemming, 2003). Moreover, the C-terminal regulatory hydrophobic region of AKT possesses a conserved serine residue essential for kinase phosphorylation and subsequent activation (Barnett et al., 2005). These isoforms share approximately 80% homology in their amino acid sequences and exhibit specific functions (Dummler and Hemmings, 2007). AKT1 primarily regulates cell growth and division, while AKT2 plays a significant role in cellular energy and metabolism (Zhou et al., 2006). AKT3, the least studied isoform, has been implicated in brain development and the viability of malignant glioma cells (Easton et al., 2005).

Aberrant expression of AKT has been observed in various human cancers, including breast, lung, ovarian, pancreatic, and gastric carcinomas (Shi et al., 2005). AKT1 amplification is commonly reported in cancer, distinguishing it from other AKT isoforms. However, activating somatic mutations in the pleckstrin homology (PH) domain of AKT1 have been identified in breast, ovarian, and colorectal cancers (Carpten et al., 2007). AKT2 amplification is more frequent in high-grade ovarian tumors and is associated with a poor prognosis for patients (Kroeger and Drapkin et al., 2017). Moreover, overexpression of AKT2 has been shown to enhance invasion and metastasis in breast and ovarian cancer cells (Arboleda et al., 2003). In a recent study using targeted exome-sequencing, a novel AKT3 mutation was discovered in a breast cancer patient with HER2 amplification and acquired resistance to trastuzumab (Carmona et al., 2016). Additionally, 20% of ovarian tumor subtypes and 40% of primary melanomas exhibited increased AKT3 expression (Easton et al., 2005; Cristiano et al., 2006). AKT3 induces G2/M transition during cell cycle progression in ovarian cancer cell lines (Cristiano et al., 2005). Inhibiting AKT as the central component of frequently disrupted PI3K/AKT signaling has long been an attractive therapeutic approach in cancer. There are two classes of AKT inhibitors: ATP-competitive and allosteric inhibitors. The ATP-competitive inhibitors bind to the active site of AKT, blocking ATP binding, whereas allosteric inhibitors bind to the PH domain, preventing AKT phosphorylation and activation (Bhutani et al., 2013). Although the three AKT isoforms have structural similarities, there are differences in their functions, tissue distribution, and substrate specificity (Fortier et al., 2011).

B-cell lymphoma-extra-large (Bcl-xL)

Accurate regulation of the intrinsic apoptotic pathway is crucial for normal development and physiology of multicellular organisms, primarily governed by the B-cell lymphoma 2 (Bcl-2) family of proteins. At the core of this pathway are the pro-survival Bcl-2 proteins (Bcl-xL, Bcl-2, Bcl-w, Bfl-1, Mcl-1), which prevent apoptosis by directly interacting with their pro-apoptotic counterparts, the effector proteins Bax, Bak (and possibly Bok), or the upstream initiators of the pathway, the BH3-only proteins (Bim, Puma, Bid, Noxa, Bad, Bmf, Hrk, Bik) (Czabotar et al., 2014). Initially discovered due to abnormal expression in B-cell lymphomas (Clearly et al., 1986; Tsujimoto and Croce, 1986; Tsujimoto et al., 1984), Bcl-2 protein's pro-survival function was demonstrated through landmark experiments, marking the separation of cell survival from proliferation pathways (Muchmore et al., 1996).

Structural studies of its relative, B-cell lymphoma-extra-large (Bcl-xL), have provided significant insights into the molecular mechanisms regulating the intrinsic apoptosis pathway. Cloned in 1993, BCL-X shares similarities with BCL-2, and its three-dimensional structure, the first among Bcl-2 family proteins, revealed eight alpha helical regions (α1-α8) (Muchmore et al., 1996). Notably, Bcl-xL, unlike other pro-survival proteins, directly interacts with cytosolic p53, influencing p53-induced apoptosis in response to stimuli like DNA damage, with implications for cancer prevention and treatment. In such scenarios, nuclear p53 upregulates p53 upregulated modulator of apoptosis (PUMA), engaging Bcl-xL, leading to p53 release and subsequent activation of Bax (Chipuk et al., 2005; Chipuk et al., 2004). Bcl-xL also interacts with non-core Bcl-2 family proteins like voltage-dependent anion channel 1, and ryanodine receptors,

impacting intracellular calcium flux (Gabellini et al., 2017; Monaco et al., 2015; Vervliet et al., 2015). While these interactions involve the Bcl-xL BH4 domain, the precise regulatory mechanism remains unclear, emphasizing the potential utility of complex structures to unravel these molecular details.

Caspase-9 (CASP9)

Procaspase-9, the initial caspase in the intrinsic apoptosis pathway, is present in a monomeric form and features an extensive prodomain housing a caspase activation domain (CARD) motif. This motif, located at the N-terminus of the prodomain, facilitates the recruitment and activation of caspase-9 at a multiprotein platform. The ensuing activation leads to the fragmentation of cells into apoptotic bodies (Bratton and Salvesen 2010). The CARD motif in the prodomain selectively binds to the Apaf-1 CARD through homotypic interactions (Qin et al.,1999). Interestingly, the autoprocessing of procaspase-9 is not intended to directly activate the caspase but serves as a molecular timer, influencing the duration of apoptosome activity (Malladi et al., 2009). Caspase-9 is constitutively expressed in various mammalian tissues, and its abnormal suppression can lead to developmental abnormalities. Research using genetic knockout techniques has revealed that mice without caspase-9 experience perinatal death accompanied by significant brain abnormalities. Caspase-9 causes the inhibition of apoptosis during brain development (Hakem et al., 1998; Kuida et al., 1998). The functional polymorphisms and subsequent disruption of the intrinsic apoptosis pathway in the caspase-9 gene are connected and increase susceptibility to various cancers, consisting of lung, bladder, pancreatic, colorectal, and gastric cancers (Park et al., 2006; Gangwar et al., 2009; Theodoropoulos et al., 2010; Liamarkopoulos et al., 2011; Theodoropoulos et al., 2011).

In the later stages of Huntington's disease, there's an observed presence of activated caspase-9 and caspase-3 activities. This suggests that apoptosis might play a role in the neuronal death that occurs during this advanced phase of the disease, as indicated by (Kiechle et al., 2002). The findings support the idea that caspase-9 plays a crucial role in maintaining cell balance by cleaving key components associated with apoptosis. Caspase-9 is like the maestro in charge of orchestrating cell death, especially in the early stages of development. It plays a crucial role in keeping abnormal cells in check throughout an organism's life. Some recent investigations have identified three tiny but mighty players—miRNA-24a, miRNA-582-5p, and miRNA-23a. These little guys have the power to put the brakes on caspase-9 activation, essentially stopping cells from going down the path of mitochondrial apoptosis. Through experiments like reporter assays and loss-of-function studies, scientists have found that when miRNA-24a is missing, caspase-9 protein levels go up, but oddly enough, mRNA levels stay the same. This discovery gives us a sneak peek into how miRNA-24a pulls the strings and influences caspase-9 activity. Importantly, the knockdown phenotype of miRNA is dependent on the functioning of caspase-9, highlighting miRNA-24a as a critical regulator and inhibitor of caspase-9 and programmed cell death, as reported by (Walker et al., 2009).

There's some intriguing evidence suggesting that caspase-9 could be influenced in different ways under various health conditions, opening the possibility of using it as a potential therapeutic tool. This is especially interesting because inhibiting caspase-9 activity might help combat chemotherapeutic resistance in certain types of human cancer cell lines (Kuwahara et al., 2003; Mueller et al., 2003; Oudejans et al., 2005; Wu and Ding, 2002). It turns out that when it comes to DNA damage-induced neural precursor cell death,

caspase-9 is in the mix, and interestingly, there's no noticeable loss of cytochrome c from mitochondria. This suggests that caspase-9 can directly pull the trigger as an apoptotic effector molecule (D'Sa-Eipper et al., 2001). The idea of selectively inducing apoptosis in cancer cells has long been a goal for researchers fighting cancer. So, as we continue delving into the activation, function, and regulation of caspase-9, it looks like it might become not just a potential treatment for cancer but also a target for addressing degenerative and developmental disorders.

Beta-Actin (ACTB)

Beta-actin (ACTB), a highly conserved cytoskeletal protein, is abundant in all eukaryotic cells. It plays crucial roles in various cellular processes, including cell migration, cell division, embryonic development, wound healing, immune response, and gene expression (Waxman and Wurmbach, 2007; Bunnell et al., 2011; Ruan et al., 2007; Nowak et al., 2002). ACTB's functional versatility stems from its capacity to form dynamic filaments that can swiftly assemble and disassemble in response to cellular requirements (Bunnell et al., 2011; Ruan et al., 2007; Polard and Borisy, 2003). Traditionally considered a constitutive housekeeping gene, ACTB expression is often assumed to remain unaffected by various experimental or physiological conditions. Consequently, it has been widely employed as a reference for quantifying changes within gene/protein expression in cells and tissues (Le et al., 1998; Micheva et al., 1998; Micheva et al., 1998). In liver cancer tissues, ACTB exhibits up-regulation. Studies utilizing gene microarray and quantitative real-time RT-PCR (qRT-PCR) techniques have demonstrated a two- to three-fold up-regulation of ACTB in advanced stages of HCV-induced hepatocellular carcinoma (HCC) (Waxman and Wurmbach, 2007). Furthermore, analysis of ACTB gene levels in normal

liver tissues and paired tumor and non-tumor tissues of HBV-related HCC patients has revealed differential expression, highlighting the potential for misinterpretation of gene expression findings (Fu et al., 2009). ACTB has been implicated in the invasiveness of melanoma cells. Analysis of cDNA arrays comparing gene expression in two melanoma cell lines, 1C8 (non-invasive) and T1C3 (invasive), derived from the same patient, revealed a twofold higher mRNA level of ACTB in the invasive T1C3 cells compared to the non-invasive 1C8 cells (Goidin et al., 2001).

Prostate cancer stands as a significant contributor to cancer-related deaths in men, emphasizing the importance of early detection and prompt treatment of localized disease (Mori et al., 2008). qRT-PCR analysis demonstrated higher expression of ACTB in human formalin-fixed paraffin-embedded (FFPE) prostate cancer tissues compared to matched peritumoral normal tissues obtained through laser microdissection (Mori et al., 2008; Ohl et al., 2005). Consequently, due to its dysregulation in prostate cancer, ACTB is deemed unsuitable for normalization purposes in gene profiling studies involving normal and malignant prostate tissues (Ohl et al., 2005). The polymerization of ACTB and the formation of its cytoskeleton contribute to cell protrusions and motility, suggesting that overexpression of ACTB may enhance cancer cell motility. ACTB mRNA was found to be localized in various cancer cell types, where active ACTB polymerization occurs. This localization ability of ACTB mRNA was correlated with efficient cell motility. Moreover, the accumulation of ACTB mRNA localization was associated with the metastatic potential of cancer cells, as delocalization of ACTB mRNA from cell leading edges led to the loss of cell polarity and directional movement. Notably, ACTB expression was significantly up regulated in highly invasive variants of different tumor cell lines, supporting the

involvement of ACTB in tumor metastasis (Nowak et al., 2002; Le et al., 1998; Popow et al., 2006; Nowak et al., 2005).

CHAPTER 3

DESIGN OF THE STUDY

Identification of miRNAs (hsa-miR-3202 and hsa-miR-7152)

microRNAs (miRNAs) regulate the mRNAs of multiple genes, including transcription factors that activate gene expression at the DNA level through binding to consensus sequences in the promoter region of a gene. miRNAs impede translation and promote degradation of mRNAs of target genes. The information available at the National Center for Biotechnology Information (NCBI) and University of California Santa Cruz (UCSC) Genome Browser was used to identify genes involved in splicing of pre-mRNA. At the miRBase database, several miRNAs of interest were identified and two of the miRNAs were selected for the study, hsa-miR-3202 and hsa-miR-7152. The nucleotide sequence of hsa-miR-3202 and hsa-miR-7152 were used to deduce the extended nucleotide sequence around the pre-miRNA nucleotide sequence using the UCSC Genome Browser and NCBI database. Forward and reverse primers were designed based on the extended pre-miRNA sequence using AmplifX 1.1 software (http://crn2m.univ-mrs.fr/pub/amplifx-dist) designed by Nicolas Jullien at the Centre for Research in Neurobiology and Neurophysiology of Marseille (CNRS), Aix-Marseille University. In addition, Sequencher 5.0 software (Gene Codes Corporation, Ann Arbor, MI) was used to analyze and identify restriction enzyme sites for cutters and non-cutters within the restriction enzyme-tagged pre-hsa-miR-3202 and pre-hsa-miR-7152 nucleotide sequences to avoid using restriction

enzymes that cut either within the restriction enzyme tagged sites or inside the hsa-miR-3202 and hsa-miR-7152 stem-loops. The forward and reverse primer sequences were modified and tagged with additional restriction enzyme sites, and the primers were synthesized (Sigma Aldrich, St. Louis, MO).

Polymerase Chain Reaction (PCR) and Gel Electrophoresis (hsa-miR-3202 and hsa-miR-7152)

The designed primers were used for polymerase chain reaction (PCR) on cDNA templates. The total volume of the PCR reaction mixture was 15.0 µL and contained 2.5 µL of DNA, or cDNA (250 ng), 7.5 µL of HotStar Taq Master Mix (Qiagen, Valencia, CA), 1.0 µL (10 nM) of forward primer, 1.0 µL (10 nM) of reverse primer and 3 µl of nuclease free H2O). PCR was carried out using a BioRad C1000 Touch machine (BioRad, Hercules, CA), and the PCR conditions were as follows: 95°C for 15 min, followed by 45 cycles of 94°C for 45 sec, 60°C for 30 sec, 72°C for 60 sec, and ending with 72°C for 10 minutes. Analysis of the amplified PCR product was completed for 5.0 µL samples on a 2% agarose gel stained with ethidium bromide and visualized in a Li-COR Odyssey® Fc imager (LI-COR Biosciences, Lincoln, NE).

Cloning of PCR-product into pCR™4-TOPO® TA vector (hsa-miR-4259)

The PCR-product of hsa-miR-3202 and hsa-miR-7152 was ligated into 4-TOPO vector using pCR™4-TOPO® TA Vector for sequencing (Life Technology, Grand Island, NY) according to the manufacturer's protocol. The resulting recombinant products were used to transform competent F10 Escherichia coli (E. coli) cells, which were then plated on LB kanamycin/X-gal agar plates for blue /white colony selection. The plates were

incubated in a Forced Air General Incubator (VWR, Radnor, PA) overnight (18 hours) at 37°C. Finally, four single white colonies were picked and dissolved in water. The dissolved single colonies were used for PCR using the procedure described in the PCR section above.

Isolation of hsa-miR-3202 and hsa-miR-7152-DNA Constructs; Restriction Enzyme Digestion; and Direct DNA Sequencing

Colonies positive by PCR analysis were cultured in LB kanamycin broth and incubated, with shaking at 250 revolutions per minute (rpm), in a Forced Air General Incubator (VWR, Radnor, PA) overnight (18 hrs) at 37°C. Pre-hsa-miR-3202-4-TOPO and pre-hsa-miR-7152-4-TOPO DNA plasmids were isolated from the LB kanamycin broth using a Plasmid DNA Miniprep Kit (Qiagen, Valencia, CA) according to the manufacturer's protocol. The isolated pre-hsa-miR-3202-4-TOPO and pre-hsa-miR-7152-4-TOPO DNA constructs were tested for the presence of a pre-hsa-miRNA-4259 fragment by PCR. After PCR confirmation, the pre-hsa-miR-3202-4-TOPO and pre-hsa-miR-7152-4-TOPO DNAs were digested with restriction enzymes in a total volume of 100 µL, containing 5.0 µg of plasmid DNA, 10 µL of 10X restriction enzyme digestion buffer, 100 units of Bam HI and 100 units of Hind III (New England BioLabs, Ipswich, MA) according to the manufacturer's protocol. Digested pre-hsa-miR-3202-4-TOPO and pre-hsa-miR-7152-4-TOPO DNAs were analyzed on a 2% low melting agarose gel stained with ethidium bromide and visualized using a Li-COR Odyssey® Fc imager (LI-COR Biosciences, Lincoln, NE). The pre-hsa-miR-3202 and pre-hsa-miR-7152 fragments were excised from the gel and purified using Geneclean (MP Biolab, Solon, OH) according to the manufacturer's protocol. The purified pre-hsa-miR-3202 and pre-hsa-miR-7152 fragments were further ligated into pmR-ZsGreen1 expression vector, a green fluorescence

protein (GFP) vector (Clontech, Mountain View, CA) according to the manufacturer's protocol. The ligated pre-hsa-miR-3202-GFP DNA was used to transform competent DH5α E. coli cells (New England BioLabs, Ipswich, MA) according to the manufacturer's protocol. The cells were plated on LB kanamycin agar plates that were incubated in a Forced Air General Incubator (VWR, Radnor, PA) at 37°C overnight (18 hrs). Two to four single colonies were picked from the plates and plasmid DNA was isolated as previously described. The plasmid DNA was tested for the presence of pre-miRNA fragments by PCR as described in the PCR section. The pre-hsa-miR-3202-GFP DNA and pre-hsa-miR-7152-GFP DNA constructs were digested with restriction enzymes in a total volume of 20 µL, containing 0.50 µg of DNA, 2 µl of 10X restriction enzyme digestion buffer, 20 units of Bam HI and 20 units of Hind III (New England BioLabs, Ipswich, MA) according to the manufacturer's protocol. The digested DNA was analyzed on a 2% agarose gel stained with ethidium bromide and visualized using a Li-COR Odyssey® Fc imager (LI-COR Biosciences, Lincoln, NE), and the pre-hsa-miR-3202-GFP DNA and pre-hsa-miR-7152-GFP DNA constructs were sequenced at the MD Anderson Cancer Center (MDACC) Sequencing and Microarray Facility (MDACC SMF, Houston, TX).

Transient Transfection of Pre-hsa-miR-3202-GFP DNA and Pre-hsa-miR-7152-GFP DNA Constructs into PC-3 cells

To culture the PC-3 cells (ATCC, Manassas, VA), 2.50 x 106 cells were seeded in ten 60 x15 mm cell cultured plates (a total of 10 plates were used, four plates were used as controls and six plates were used for the transient transfections), containing Dulbecco's Modified Eagle Medium (DMEM) supplemented with, L-glutamine, 1% GlutaMAX, 10% fetal bovine serum (FBS), and 1% penicillin and streptomycin (Life Technologies, Grand

Island, NY). The PC-3 cells were incubated in a 5% CO2 incubator at 37°C for 24 hours (h). The PC-3 cells were allowed to reach 80-90% confluence before transfections were performed. Transient transfections were performed using pre-hsa-miR-3202-pmR-ZsGreen1 and pre-hsa-miR-7152-pmR-ZsGreen1 DNA constructs and mock transfections were also performed with/without the plasmid vector DNA, which serves as the controls. For the experimental sets, 5.0 µg of pre-hsa-miR-3202-pmR-ZsGreen1 and pre-hsa-miR-7152-pmR-ZsGreen1 DNA constructs were treated with lipofectamine 2000 reagent (Life Technologies, Grand Island, NY) according to the manufacturer's protocol. A 96h course of three 24 h intervals of transient-transfection experiments were performed in which individually 5.0 µg of pre-hsa-miR-3202-pmR-ZsGreen1 and pre-hsa-miR-7152-pmR-ZsGreen1 DNA constructs treated with lipofectamine 2000 were transient-transfected into the PC-3 cells. At the time course of 24 h, 48 h, and 96 h, the treated transient-transfected and mock-transfected PC-3 cells were harvested.

Treatment of LY2835219, LEE011 and Palbociclib into PC-3 cells

To culture the PC-3 cells (ATCC, Manassas, VA), 2.50 x 106 cells were seeded in ten 60 x15 mm cell cultured plates (a total of 15 plates were used, six plates were used as controls and nine plates were used for treatment), containing Dulbecco's Modified Eagle Medium (DMEM) supplemented with, L-glutamine, 1% GlutaMAX, 10% fetal bovine serum (FBS), and 1% penicillin and streptomycin (Life Technologies, Grand Island, NY). The PC-3 cells were incubated in a 5% CO2 incubator at 37°C for 24 hours (h). The PC-3 cells were allowed to reach 80-90% confluence before treatments were performed. Treatments were performed using LY2835219, LEE011, and Palbociclib, and mock transfections were also performed with/without the plasmid vector DNA, which serves as

the controls. For the experimental sets, 151.937 µl of LY2835219, 165.791 µl of LEE011, and 172.632 µl of Palbociclib were treated to the set of plates based on the half-lethal dosage of each (MedChemExpress, Monmouth Junction, NJ) according to the manufacturer's protocol. A 96 h course of three 24 h intervals of experiments were performed in which individually LY2835219, LEE011, and Palbociclib were treated into PC-3 cells. At the time course of 24 h, 48 h, and 96 h, the treated transient-transfected and mock-transfected PC-3 cells were harvested.

Microscopic Visualization of Cells Proliferation

The controls and the treated PC-3 cells in the tissue-culture dishes were visualized under the Eclipse Ti-E Inverted Nikon Microscope, (Nikon Instruments Inc., Melville, NY). Proliferation of the cells was determined and analyzed to whether it occurred or not. Photos of the PC-3 cells in the individual tissue-culture dishes were captured at both Superimposed and 10X Phase Contrast Magnification.

Isolation of Protein

The proteins from PC-3 cells underwent isolation using the Radio-Immunoprecipitation Assay (RIPA) reagent (Cell Signaling in Danvers, MA). Subsequently, the cell media from each culture dish was meticulously harvested and swiftly centrifuged to concentrate cellular constituents. The cells in each dish were treated with 1X RIPA lysis buffer enriched with 1 mM phenylmethanesulfonylfluoride fluoride (PMSF), protease inhibitor (1:100), and protease I phosphate inhibitor (1:100) (Cell Signaling in Beverly, MA), following the manufacturer's guidelines. The cells, now immersed in the RIPA lysis buffer, were detached from the dish, and put in individual 1.5

mL microcentrifuge tubes, where they were gently tapped multiple times. Each microcentrifuge tube, housing the lysed cells, sat on ice for precisely 45 minutes. Then a microcentrifuge operating at 4 degrees Celsius spun at 14,000 revolutions per minute (rpm) for 20 minutes, effectively segregating cellular debris to the tube's bottom while retaining the aqueous proteins above. Following the 20-minute centrifugation stint at 4°C, the aqueous transitioned into fresh 1.5 mL microcentrifuge tubes. These extracted proteins were then preserved at -80°C, ensuring optimal storage conditions for subsequent analyses.

Reading of Optical Density 280 (OD_{280}) for Proteins Isolated

To quantify the extracted proteins, the Optical Density at 280 nm (OD280) was determined, with the Spectronic BioMate 3 UV-Vis instrument (Thermofisher™ in Waltham, MA), serving to validate each experimental protein sample. In this process, 2.5 microliters (µl) of the extracted proteins were carefully withdrawn from each experimental protein sample and introduced to 997.5 µl of UltraPure™ DNase/RNase-Free Distilled Water (Thermofisher™), residing in individual 1.5 mL microcentrifuge tubes. Tapping the tubes ensured the mixture of the proteins and distilled water. Following this mixing, each protein with distilled water was placed in an optical density reading cuvette, where the OD280 of the experimental protein sample was measured and recorded. For practicality, each experimental protein sample was aliquoted into individual 0.6 mL microcentrifuge tubes, securing their place as working stock in the -80°C freezer, ready for future use.

Western Blot and Gel Electrophoresis of Protein

The extracted protein samples unfolded with 10% Sodium Dodecyl Sulfate Polyacrylamide Gel Electrophoresis (SDS-PAGE) gels, by the BIORAD Mini-PROTEAN

Tetra System from (BIORAD in Hercules, CA), following the precise BIORAD protocol. In this protein ballet, a loading of 100 micrograms (µg) of each individually extracted protein sample transpired into its designated well within the 10% SDS-PAGE gel. The Precision Plus Protein™ WesternC™ Blotting Standard from BIORAD, a marker, was added in a separate well. The ensemble of 10% SDS-PAGE gels with experimental protein samples, ran according to the BIORAD protocol. Multiple SDS-PAGE gels were run simultaneously. These 10% SDS-PAGE gels were later employed in both coomassie blue dye staining and Western blotting experiments, adding layers of insight to the ongoing investigation.

For the Western blotting experiments, the proteins that ran through the 10% SDS-PAGE gel were placed on nitrocellulose membranes to be transferred using the Trans-Blot® Turbo™ Transfer System (BIORAD in Hercules, CA), following the intricate BIORAD protocol. On the nitrocellulose membranes, the proteins were probed with either Primary Rabbit or Mouse IgG HRP-linked antibodies, and further embellished with Secondary Anti-Rabbit or Anti-Mouse IgG HRP-linked antibodies. The antibodies used were ACTB, Bcl-xL, and CDK4, which were specifically probed with polyclonal rabbit or mouse IgG HRP-linked antibodies (Cell Signaling, Danvers, MA) following Cell Signaling's protocol. The probing of proteins featured a primary polyclonal rabbit CCND1, AKT, and CASP9 IgG, HRP-linked antibodies, with a subsequent secondary Goat Anti-Rabbit IgG H&L (HRP) antibody (Abcam Cambridge, MA), as per Abcam's meticulous protocol. In the final part of the Western blotting experiments, the antibody-treated nitrocellulose membranes were developed using Clarity™ and Clarity Max™ Western (ECL) Blotting Substrates (BIO-RAD in Hercules, CA). Following the meticulous script

provided by BIO-RAD's protocol, these substrates unfolded a chemiluminescent detection mechanism, unveiling the protein bands within a chemiluminescence imaging system. The substrate-treated nitrocellulose membranes with the luminescence of detected proteins, were viewed under the Li-COR Odyssey® Fc imager (LI-COR Biosciences in Lincoln, NE). The protein bands and expressions were detected. The trimmed intensity signal in this software, excluding five percent of pixels with the highest and lowest pixel intensity from the total pixel intensity signals, was the metric employed to quantify the intensity of each protein band.

CHAPTER 4

RESULTS AND DISCUSSION

Transient Transfection of miRs on PC-3 Cells

Once seeding the PC-3 cells transient transfection was performed using both pre-hsa-miR-3202-pmR-ZsGreen1 and pre-hsa-miR-7152-pmR-ZsGreen1 DNA Constructs over 96 hours (h) to observe the effect it would have. Both 24 h untreated controls (Figure 1A and 2A) and 24 h GFP Controls (Figure 1B and 2B) were used before transient transfection took place. Observing the PC-3 cells at each interval of 24 h for a total of 96 h it showed the plates of PC-3 cells containing hsa-miR-3202-pmR-ZsGreen1 DNA construct and hsa-miR-7152-pmR-ZsGreen1 DNA construct proliferated overtime for 96 h (Figure 1C, 1D, 1E, 2C, 2D and 2E). This observation showed that the miRs in point do not cause apoptosis to the cells however, they could still regulate genes in both the cell cycle and proliferation pathway carrying out protein experiments.

Treatment of Drugs on PC-3 Cells

Once the PC-3 cells were seeded in the plates they were treated with three different drugs, LY2835219, LEE001, and Palbociclib at half-lethal dosage throughout 96 h to observe the effect it would have on the cells. A 24 h untreated control was used before the treatment of each drug (Figure 3A, 4A, and 5A). Observing the plates containing the treated PC-3 Cells at each interval of 24 h showed that the drugs killed off at least 50 percent of the cells by 96 h (Figure 3B, 3C, 3D, 4B, 4C, 4D, 5B, 5C and 5D) as compared to the PC-

3 cells that were transient transfected with the miRs. This observation could prove to show that the drugs act on the cells to cause cell death as well as play a role in cell cycle regulation. This will be proven by carrying out protein experiments.

Expression of Protein

Cyclin D1 (CCND1) is important in cell cycle regulation by interacting with the cyclin-dependent kinase 4 (CDK4) that can cause an uncontrol proliferation of cells that can lead to tumors and cancers. LY2835219 is known to be a potent target to act on both CCND1 and CDK4, while both LEE001 and Palbociclib target CDK4. All three drugs act on both these cell cycle regulators to stop their interaction to carry out the cell cycle process. Both hsa-miR-3202 and hsa-miR-7152 target CCND1 and CDK4 respectively as determined by the miR database. Looking at the western blot results for LY2835219 it showed a down-regulation of CCND1 protein expression at 24 h with the bar graph showing the protein expression of CCND1 with both the trimmed signal values and standard error bars (Figure 6A and 6C), while hsa-miR-3202 showed a down-regulation of CCND1 protein expression after 24 h with the bar graph showing the protein expression of CCND1 with trimmed signal values and standard error bars (Figure 6B and 6C). Both results were compared, and this showed that LY2835219 is more effective against CCND1 than hsa-miR-3202 based on the trimmed signal values being higher in hsa-miR-3202 at 24 h, 48 h, and 96 h at the protein level (Figure 6A, 6B, and 6C) as well as calculating F-statistic and P-value for the xenobiotic drug and overexpressed miR on CCND1 and carrying out One-Way ANOVA that determined that the experimental treatments compared to the control was insignificant (Table 1A and 1B). The western blot results for

LY2835219, LEE011, and Palbociclib against CDK4 were compared and it showed that after 24 h CDK4 was downregulated by all three, however looking at the bar graph containing the trimmed signal values and standard error bars for CDK4 expression, LY2835219 had a more potent effect on CDK4 followed by LEE011 and then Palbociclib (Figure 7A and 7B) at the protein level.

The western blot result for hsa-miR-7152 showed that CDK4 down-regulation did not occur until after 24 h and the expression drastically decreased after 48 h. The trimmed signal values with standard error bars for CDK4 expression were higher than in the drugs (Figure 8A and 8B). The drugs (LY2835219, LEE011, and Palbociclib) compared to hsa-miR-7152 caused a more drastic reduction in CDK4 than hsa-miR-7152 and that they are more potent on both the cell cycle regulators at the protein level. The F-statistic and P-value were calculated for the xenobiotic drugs and miRs on CDK4 and One-Way ANOVA was carried out and it was determined the experimental treatments compared to the control were insignificant (Table 2A and 2B). AKT has been known to promote cell survival directly and indirectly. Specifically, it targets Bcl-xL indirectly by disassociating BAD, which is usually attached to the Bcl-2/Bcl-xL complex to cause the loss of the pro-apoptotic function through phosphorylation. AKT is also known to regulate CASP9 by phosphorylation, which is known as the initiator caspase that helps facilitate the regulation of CASP3 to carry out apoptosis or normal cell death function. This shows that AKT is very important in regulating both the cell cycle and apoptotic pathways. Observing if both the xenobiotic drugs and overexpressed miRs will cause the downregulation of AKT and

the genes it regulates (Bcl-xL and CASP9) will open even more options in helping treat human diseases.

The western blot results for LY2835219, LEE011, and Palbociclib against AKT were compared and it showed that after 48 h AKT was downregulated by all three. When looking at the bar graph containing the trimmed signal values and standard error bars for AKT expression, LEE011 had a more potent effect on AKT followed by LY2835219 and then Palbociclib after 48 h (Figure 9A and 9B) at the protein level. The western blot result for hsa-miR-3202 and hsa-miR-7152 showed that AKT down-regulation did not occur until after 48, which was minimal. The trimmed signal values with standard error bars for AKT expression were higher than in the drugs because of the minimal effect (Figure 9A and 9B).

The drugs (LY2835219, LEE011, and Palbociclib) compared to the overexpressed miRs (hsa-miR-3202 and hsa-miR-7152) caused a more drastic reduction in AKT and that they are more potent on AKT at the protein level. The F-statistic and P-value were calculated for the xenobiotic drugs and overexpressed miRs on AKT and One-Way ANOVA was carried out and it was determined the experimental treatments compared to the control were significant (Table 3A and 3B). The western blot results for LY2835219, LEE011, and Palbociclib against Bcl-xL were compared, and it showed downregulation in all three drugs, however, LEE011 downregulation started after 24 h, whereas for both LY2835219 and Palbociclib, it began after 48 h. When looking at the bar graph containing the trimmed signal values and standard error bars for Bcl-xL expression, LEE011 had a more potent effect on Bcl-xL followed by Palbociclib and then LY2835219 (Figure 10A and 10B) at the protein level. The western blot result for hsa-miR-3202 and hsa-miR-7152

did not show much of a down-regulation for Bcl-xL. The trimmed signal values with standard error bars for Bcl-xL expression were higher than in the drugs except for the control (Figure 10A and 10B). The drugs (LY2835219, LEE011, and Palbociclib) compared to the overexpressed miRs (hsa-miR-3202 and hsa-miR-7152) caused more reduction in Bcl-xL proving that they are more potent on Bcl-xL at the protein level. The F-statistic and P-value were calculated for the xenobiotic drugs and miRs on Bcl-xL and One-Way ANOVA was carried out and it was determined the experimental treatments compared to the control were insignificant (Table 4A and 4B). The western blot results for LY2835219, LEE011, and Palbociclib against CASP9 were compared, and it showed downregulation in all three drugs after 48 h. When looking at the bar graph containing the trimmed signal values and standard error bars for CASP9 expression, LEE011 and Palbociclib had a more potent effect on CASP9 followed by LY2835219 (Figure 11A and 11B) at the protein level. The western blot result for hsa-miR-3202 and hsa-miR-7152 showed minimal down-regulation for CASP9 after 48 h. The trimmed signal values with standard error bars for CASP9 expression were higher than in the drugs (Figure 11A and 11B).

The drugs (LY2835219, LEE011, and Palbociclib) as compared to the overexpressed miRs (hsa-miR-3202 and hsa-miR-7152) caused more down expression of CASP9 making them more potent at the protein level to cause apoptosis. The F-statistic and P-value were calculated for the xenobiotic drugs and overexpressed miRs on CASP9 and One-Way ANOVA was carried out and it was determined the experimental treatments compared to the control were insignificant (Table 5A and 5B). ACTB are part of a cell's

construction and they're essential for many functions, from helping cells move around to making sure they divide correctly and even influencing which genes get turned on or off. The secret to their versatility is their ability to build and break down structures (filaments) quickly.

The western blot results for LY2835219, LEE011, and Palbociclib against ACTB were compared, and it showed a breakdown of ACTB in both LY2835219 and LEE011 after 48 h. When looking at the bar graph containing the trimmed signal values and standard error bars for ACTB expression, the 96 h treatment of LY2835219 and LEE011 was lower than the treatment in Palbociclib which could suggest that both LY2835219 and LEE011 could affect the motility, and structure of the cell (Figure 12A and 12B) at the protein level.

The western blot result for hsa-miR-3202 and hsa-miR-7152 did not show any downregulation of ACTB. The trimmed signal values with standard error bars for ACTB expression were normal for the overexpressed miRs which could mean that they do not cause any type of disturbance to the cells (Figure 12A and 12B). The drugs (LY2835219, LEE011, and Palbociclib) compared to the overexpressed miRs (hsa-miR-3202 and hsa-miR-7152) proved to cause the expression of ACTB to decrease specifically LY2835219 and LEE011 as compared to both Palbociclib and the overexpressed miRs (hsa-miR-3202 and hsa-miR-7152) making them more potent at the protein level to cause cell structure instability. The F-statistic and P-value were calculated for the xenobiotic drugs and overexpressed miRs on ACTB and One-Way ANOVA was carried out and it was determined the experimental treatments compared to the control were significant (Table 6A and 6B). The results from this study showed that the xenobiotic drugs can have a direct

effect on the PC-3 cells that accelerates the stoppage of cells dividing, causing normal cell death to occur and the breakdown of the construction of the cell's motility as compared to the overexpressed miRs that would take a much longer time to act and promote one of these three mechanisms due to them targeting only the mRNA of these cell cycle and apoptotic regulator genes.

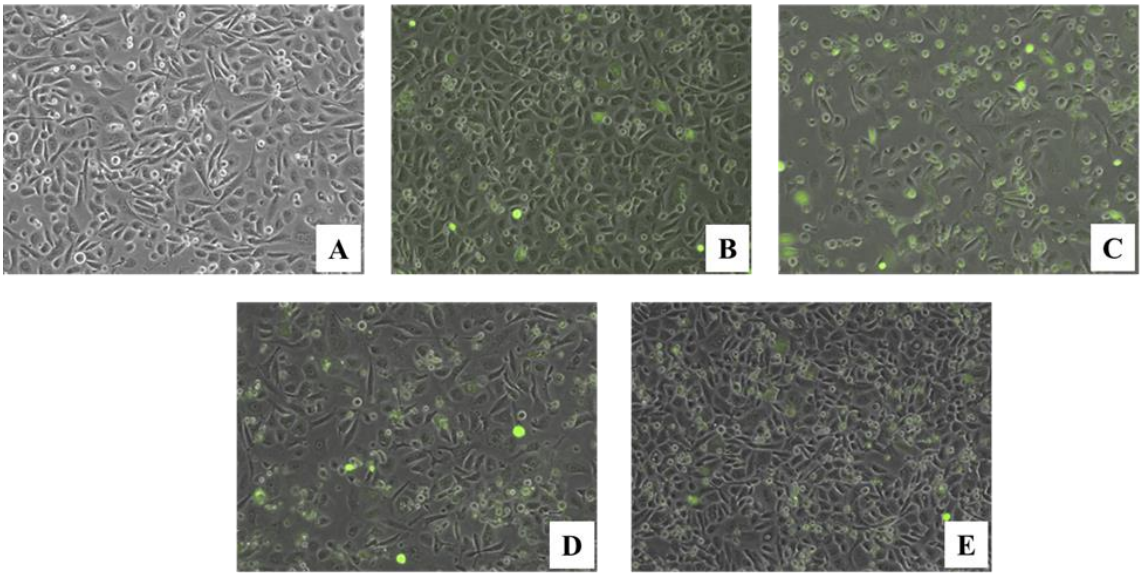

Figure 1: Expression of pre-hsa-miR-3202-pmR-ZsGreen1 DNA Construct in PC-3 Cells

The photos in **Figure 1** are labeled **A**, **B**, **C**, **D** and **E**. They show untreated PC-3 Control at 24 h, transient transfection of GFP Control at 24 h and transient transfection of hsa-miR-3202-pmR-ZsGreen1 DNA construct in PC-3 cells expressing GFP at 24 h, 48 h and 96 h. **(A)** untreated PC-3 Control 24 h, **(B)** superimposed photo of the GFP Control at 24 h **(C)** superimposed photo of the hsa-miR-3202-GFP DNA at 24 h, **(D)** superimposed photo of the hsa-miR-3202-GFP DNA at 48 h, (**E)** superimposed photo of the hsa-miR-3202-GFP DNA at 96 h.

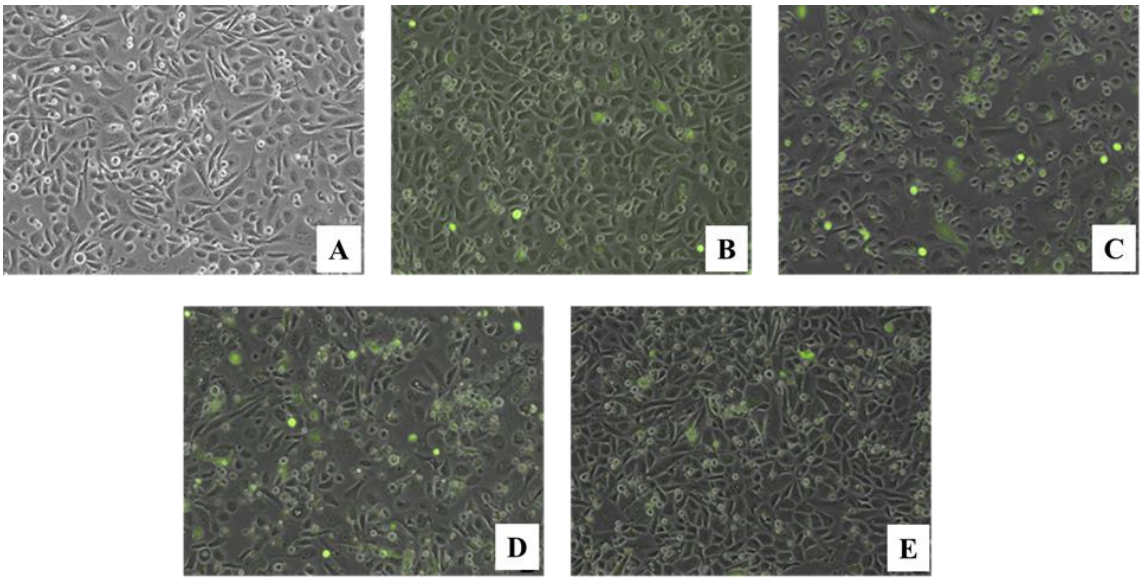

Figure 2: Expression of pre-hsa-miR-7152-pmR-ZsGreen1 DNA Construct in PC-3 Cells

The photos in **Figure 2** are labeled **A**, **B**, **C**, **D** and **E**. They show untreated PC-3 Control at 24 h, transient transfection of GFP Control at 24 h and transient transfection of hsa-miR-7152-pmR-ZsGreen1 DNA construct in PC-3 cells expressing GFP at 24 h, 48 h and 96 h. **(A)** untreated PC-3 Control 24 h, **(B)** superimposed photo of the GFP Control at 24 h **(C)** superimposed photo of the hsa-miR-7152-GFP DNA at 24 h, **(D)** superimposed photo of the hsa-miR-7152-GFP DNA at 48 h, **(E)** superimposed photo of the hsa-miR-7152-GFP DNA at 96 h.

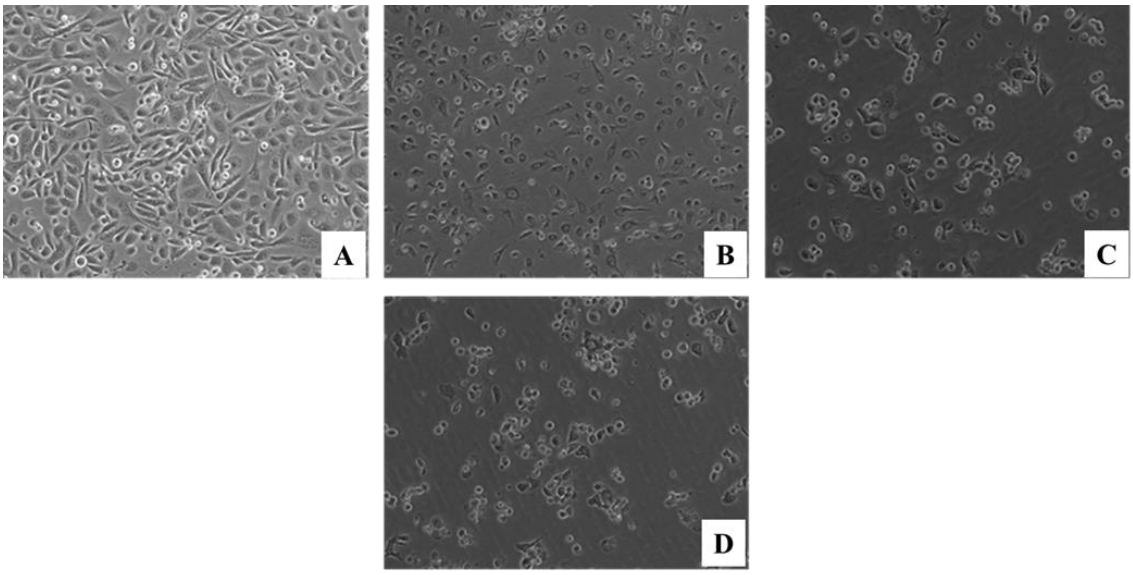

Figure 3: LY2835219 Treated PC-3 Cells

The photos in **Figure 3** are labeled **A**, **B**, **C** and **D**. They show untreated PC-3 Control at 24 h, LY2835219 treated in PC-3 cells at 24 h, 48 h and 96 h. **(A)** untreated PC-3 Control 24 h, **(B)**10X phase contrast photo of LY2835219 treated at 24 h in PC-3 cells, **(C)**10X phase contrast photo of LY2835219 treated at 48 h in PC-3 cells, **(D)** 10X phase contrast photo of LY2835219 treated at 96 h in PC-3 cells.

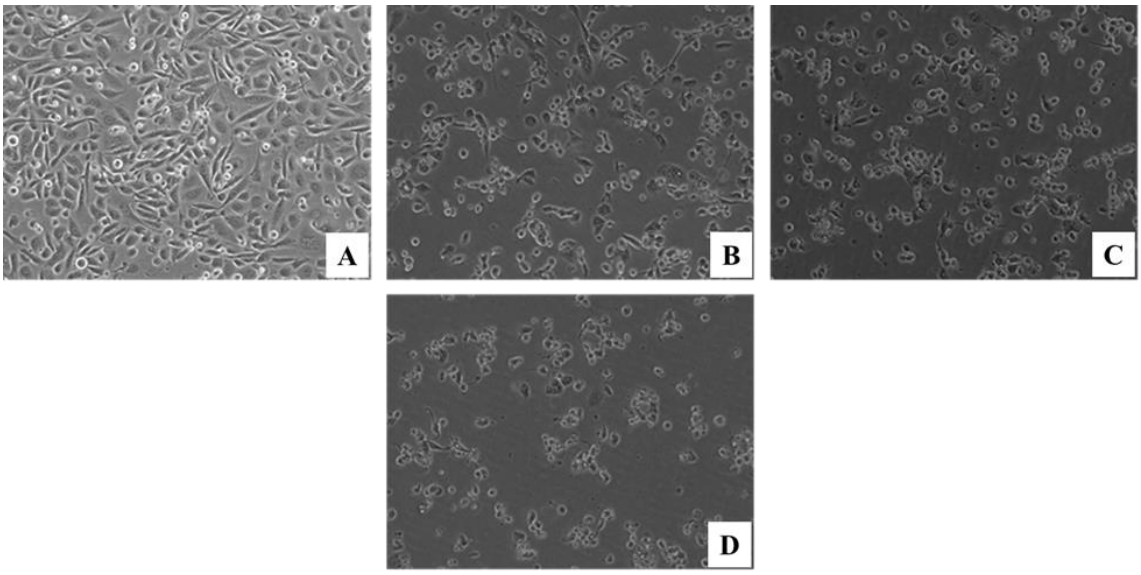

Figure 4: LEE011 Treated PC-3 Cells

The photos in **Figure 4** are labeled **A**, **B**, **C** and **D**. They show untreated PC-3 Control at 24 h, LEE011 treated in PC-3 cells at 24 h, 48 h and 96 h. **(A)** untreated PC-3 Control 24 h, **(B)**10X phase contrast photo of LEE011 treated at 24 h in PC-3 cells, **(C)**10X phase contrast photo of LEE011 treated at 48 h in PC-3 cells, **(D)** 10X phase contrast photo of LEE011 treated at 96 h in PC-3 cells.

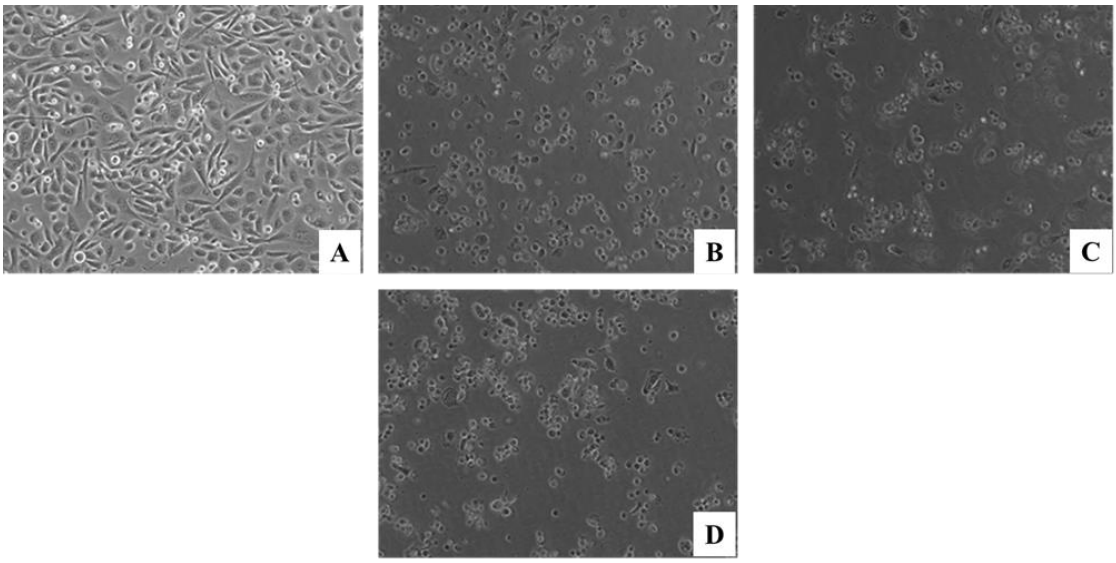

Figure 5: Palbociclib Treated PC-3 Cells

The photos in **Figure 5** are labeled **A**, **B**, **C** and **D**. They show untreated PC-3 Control at 24 h, Palbociclib treated in PC-3 cells at 24 h, 48 h and 96 h. **(A)** untreated PC-3 Control 24 h, **(B)**10X phase contrast photo of Palbociclib treated at 24 h in PC-3 cells, **(C)**10X phase contrast photo of Palbociclib treated at 48 h in PC-3 cells, **(D)** 10X phase contrast photo of Palbociclib treated at 96 h in PC-3 cells.

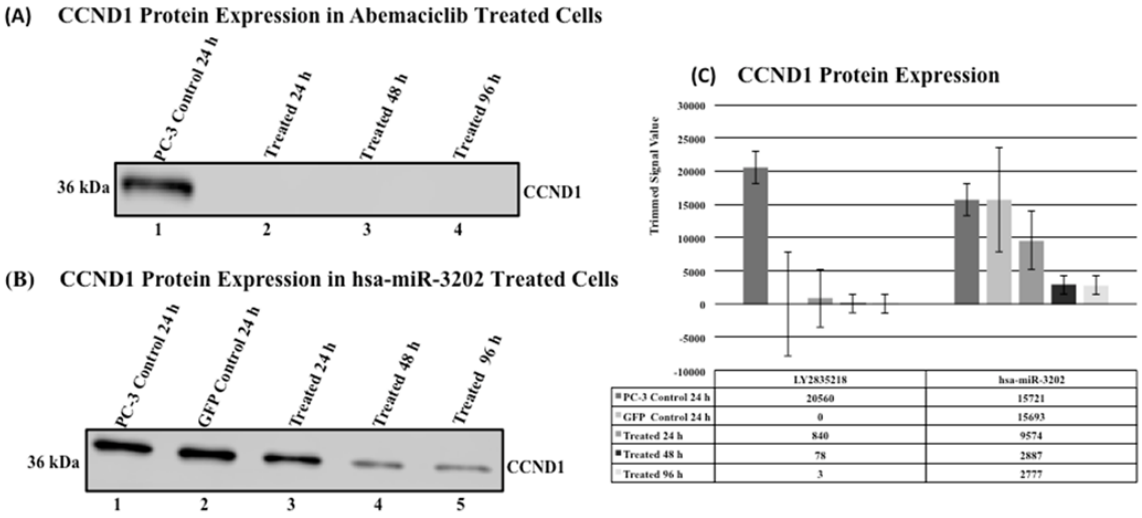

	LY2835218	hsa-miR-3202
PC-3 Control 24 h	20560	15721
GFP Control 24 h	0	15693
Treated 24 h	840	9574
Treated 48 h	78	2887
Treated 96 h	3	2777

Figure 6: Western Blot and Bar Graph Analyses Comparisons of LY2835218 and hsa-miR-3202-pmR-ZsGreen1 DNA on the Expression of CCND1

Figure 6 (A and B) Western blot protein expressions of CCDN1 in PC-3 cells that were treated with LY2835219 and transient-transfected with pre-hsa-miR-3202-pmR-ZsGreen1 DNA construct in a 24 h interval course of 96 h, including the control (i.e. mock-transfected PC-3 cells and pmR-ZsGreen1 vector DNA transient-transfected in PC-3 cells). Lane 1: PC-3 control (24 h); Lane 2: PC-3-LY2835219 Treated (24 h), PC-3-pmR-ZsGreen1vector DNA only (24 h) (hsa-miR-3202); lane 3: PC-3-LY2835219 Treated (48 h), PC-3-hsa-miR-3202-pmR-ZsGreen1 DNA (24 h); lane 4: PC-3-LY2835219 Treated (96 h), PC-3-hsa-miR-3202-pmR-ZsGreen1 DNA (48 h); lane 5: PC-3-hsa-miR-3202-pmR-ZsGreen1 DNA (96 h). **(C)** Bar Graph Comparisons showing protein expression of CCND1 at different conditon expressions for both LY2835219 and hsa-miR-3202-pmR-ZsGreen1 DNA with standard error bars and trimmed signal values.

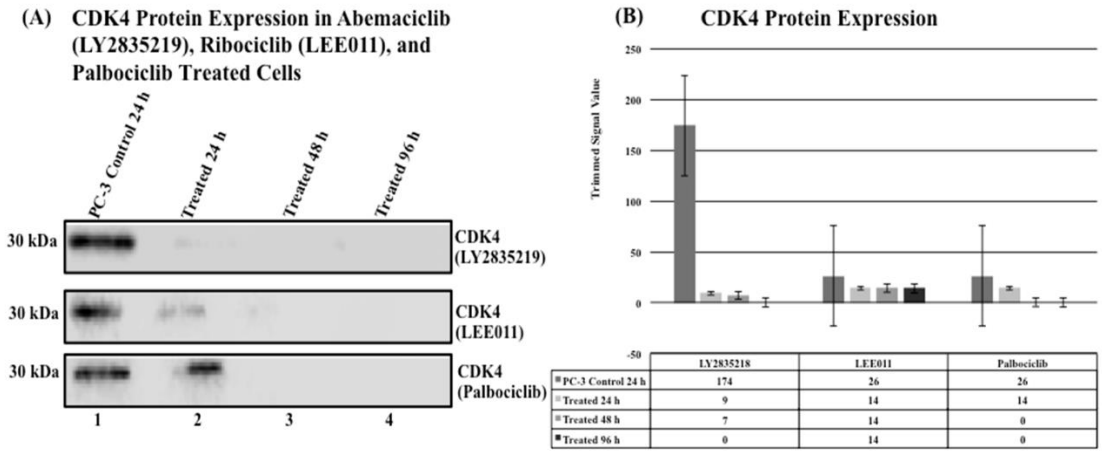

Figure 7: Western Blot and Bar Graph Analyses Comparisons of LY2835218, LEE001 and Palbociclib on the Expression of CDK4

Figure 7: **(A)** Western blot protein expressions of CDK4 in PC-3 cells that were treated with LY2835218, LEE001 and Palbociclib in a 24 h interval course of 96 h, including the control (i.e. mock-transfected PC-3 cells) Lane 1: PC-3 control (24 h); lane 2: PC-3-LY2835218, LEE011 and Palbociclib Treated (24 h); lane 3: PC-3-LY2835218, LEE011 and Palbociclib Treated (48 h); 4: PC-3-LY2835218, LEE011 and Palbociclib Treated (96 h). **(B)** Bar Graph Comparisons showing protein expression of CDK4 at different conditon expressions of LY2835219, LEE011 and Palbociclib with standard error bars and trimmed signal values.

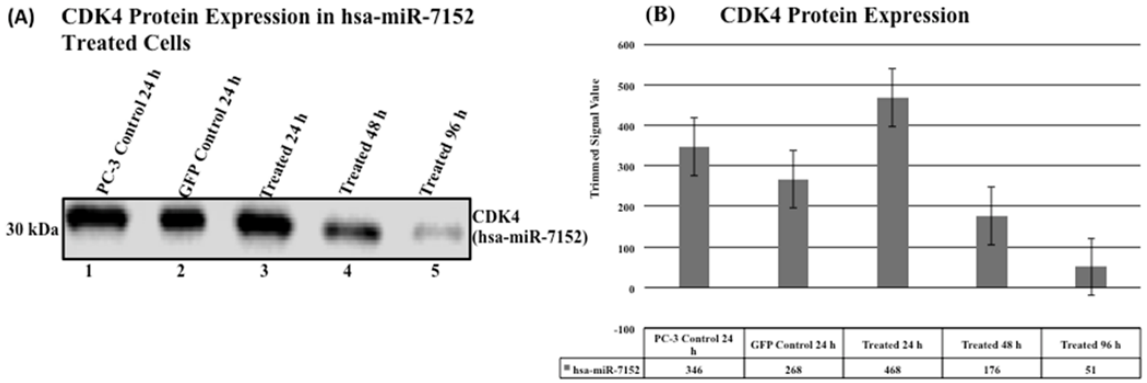

Figure 8: Western Blot and Bar Graph Analyses of hsa-miR-7152-pmR-ZsGreen1 DNA on the Expression of CDK4

Figure 8: **(A)** Western blot protein expressions of CDK4 in PC-3 cells that were transient-transfected with pre-hsa-miR-7152-pmR-ZsGreen1 DNA construct in a 24 h interval course of 96 h, including the controls (i.e. mock-transfected PC-3 cells and pmR-ZsGreen1 vector DNA transient-transfected in PC-3 cells). Lane 1: PC-3 control (24 h); lane 2: PC-3-pmR-ZsGreen1vector DNA only (24 h); lane 3: PC-3-hsa-miR-7152-pmR-ZsGreen1 DNA (24 h); lane 4: PC-3-hsa-miR-7152-pmR-ZsGreen1 DNA (48 h); lane 5: PC-3-hsa-miR-7152-pmR-ZsGreen1 DNA (96 h). **(B)** Bar Graph showing protein expression of CDK4 at different conditon expressions of hsa-miR-7152-pmR-ZsGreen1 DNA with standard error bars and trimmed signal values.

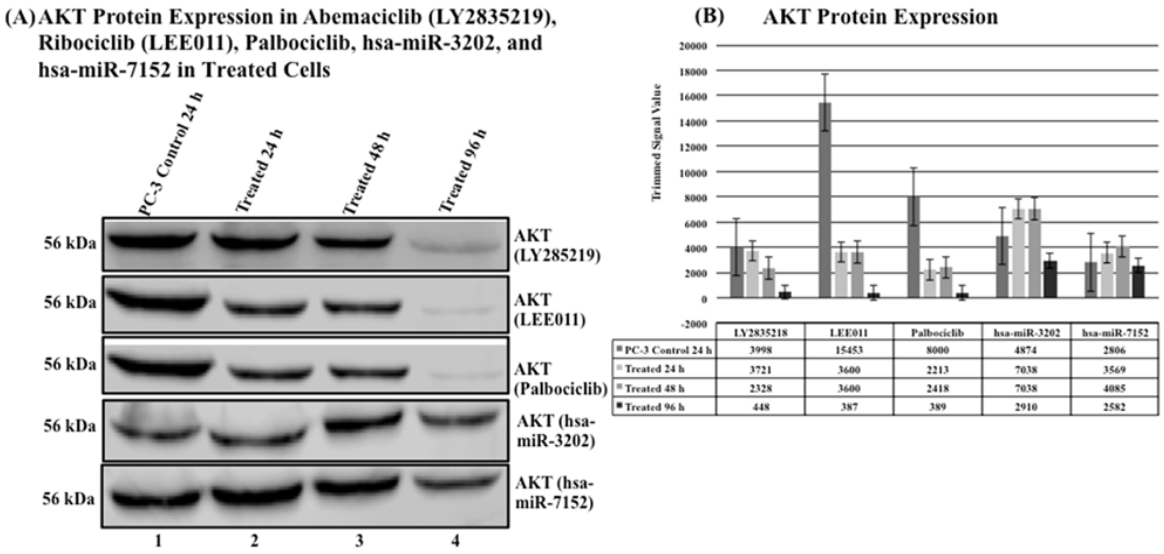

Figure 9: Western Blot and Bar Graph Analyses Comparisons of LY2835218, LEE001, Palbociclib, hsa-miR-3202-pmR-ZsGreen1 DNA and hsa-miR-7152-pmR-ZsGreen1 DNA on the Expression of AKT

Figure 9: **(A)** Western blot protein expressions of AKT in PC-3 cells that were treated with LY2835218, LEE011, Palbociclib and transient-transfected with pre-hsa-miR-3202-pmR-ZsGreen1 DNA and pre-hsa-miR-7152-pmR-ZsGreen1 DNA construct in a 24 h interval course of 96 h, including the controls (i.e. mock-transfected PC-3 cells). Lane 1: PC-3 control (24 h); lane 2: PC-3-LY2835218, LEE011 and Palbociclib Treated, PC-3-hsa-miR-3202-pmR-ZsGreen1 DNA and PC-3-hsa-miR-7152-pmR-ZsGreen1 DNA (24 h); lane 3: PC-3-LY2835218, LEE011, Palbociclib Treated, PC-3-hsa-miR-3202-pmR-ZsGreen1 DNA and PC-3-hsa-miR-7152-pmR-ZsGreen1 DNA (48 h); lane 4: PC-3-LY2835218, LEE011, Palbociclib Treated, PC-3-hsa-miR-3202-pmR-ZsGreen1 DNA and PC-3-hsa-miR-7152-pmR-ZsGreen1 DNA (96 h). **(B)** Bar Graph showing protein expression of AKT at different conditon expressions of LY2835219, LEE011, Palbociclib,

has-miR-3202-pmR-ZsGreen1 and hsa-miR-7152-pmR-ZsGreen1 DNA with standard error bars and trimmed signal values.

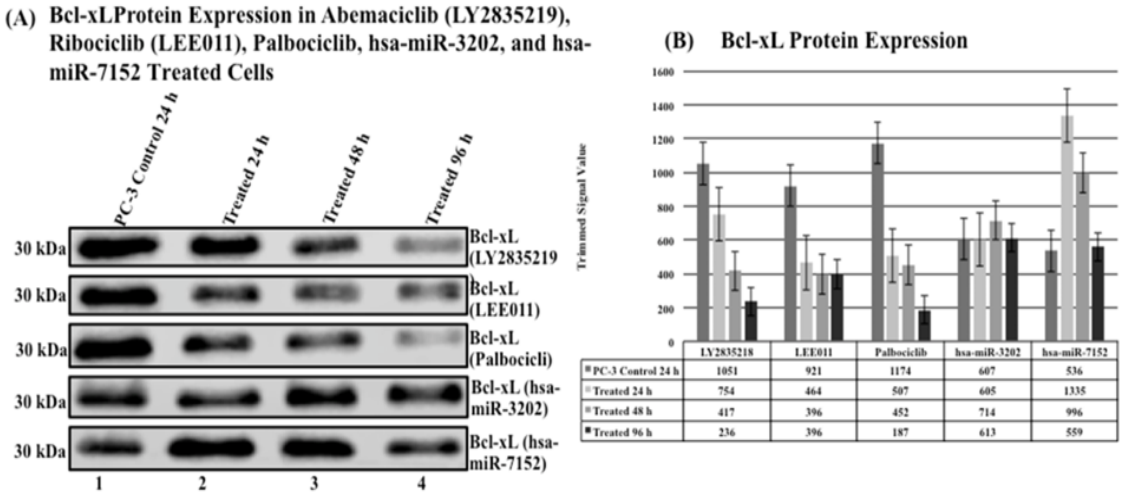

Figure 10: Western Blot and Bar Graph Analyses Comparisons of LY2835218, LEE001, Palbociclib, hsa-miR-3202-pmR-ZsGreen1 DNA and hsa-miR-7152-pmR-ZsGreen1 DNA on the Expression of Bcl-xL

Figure 10: **(A)** Western blot protein expressions of Bcl-xL in PC-3 cells that were treated with LY2835218, LEE001, Palbociclib and transient-transfected with pre-hsa-miR-3202-pmR-ZsGreen1 DNA and pre-hsa-miR-7152-pmR-ZsGreen1 DNA constructs in a 24 h interval course of 96 h, including the controls (i.e. mock-transfected PC-3 cells). Lane 1: PC-3 control (24 h); lane 2: PC-3-LY2835218, LEE011, Palbociclib Treated, PC-3-hsa-miR-3202-pmR-ZsGreen1 DNA and PC-3-hsa-miR-7152-pmR-ZsGreen1 DNA (24 h); lane 3: PC-3-LY2835218, LEE011, Palbociclib Treated, PC-3-hsa-miR-7152-pmR-ZsGreen1 DNA and PC-3-hsa-miR-7152-pmR-ZsGreen1 DNA (48 h); lane 4: PC-3-LY2835218, LEE011, Palbociclib Treated, PC-3-hsa-miR-3202-pmR-ZsGreen1 DNA and PC-3-hsa-miR-7152-pmR-ZsGreen1 DNA (96 h). **(B)** Bar Graph showing protein

expression of Bcl-xL at different conditon expressions of LY2835219, LEE011, Palbociclib, hsa-miR-3202-pmR-ZsGreen1 and hsa-miR-7152-pmR-ZsGreen1 DNA with standard error bars and trimmed signal values.

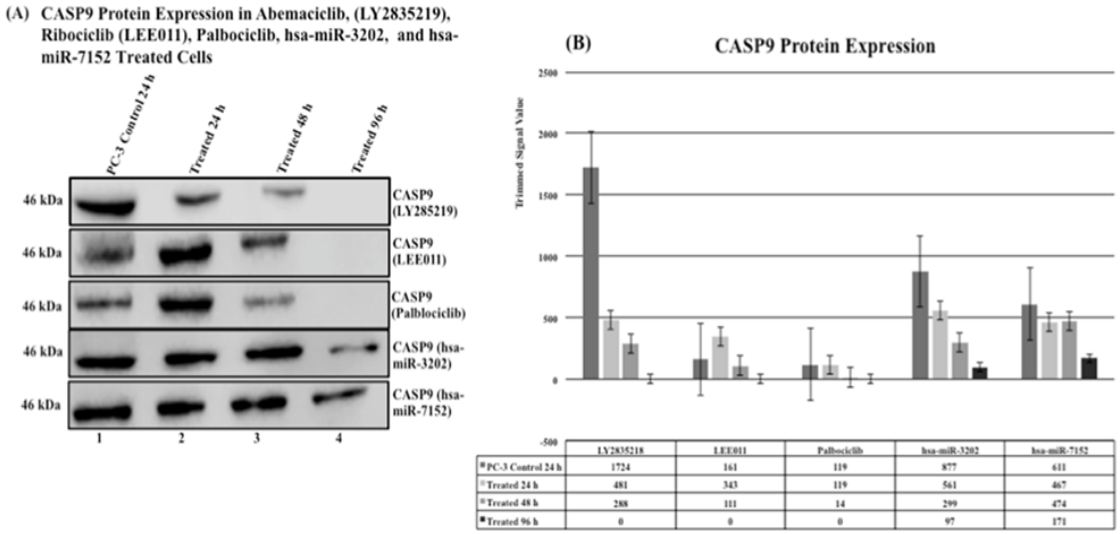

	LY2835218	LEE011	Palbociclib	hsa-miR-3202	hsa-miR-7152
PC-3 Control 24 h	1724	161	119	877	611
Treated 24 h	481	343	119	561	467
Treated 48 h	288	111	14	299	474
Treated 96 h	0	0	0	97	171

Figure 11: Western Blot and Bar Graph Analyses Comparisons of LY2835218, LEE001, Palbociclib, hsa-miR-3202-pmR-ZsGreen1 DNA and hsa-miR-7152-pmR-ZsGreen1 DNA on the Expression of CASP9

Figure 11: **(A)** Western blot protein expressions of CASP9 in PC-3 cells that were treated with LY2835218, LEE001, Palbociclib and transient-transfected with pre-hsa-miR-3202-pmR-ZsGreen1 DNA and pre-hsa-miR-7152-pmR-ZsGreen1 DNA constructs in a 24 h interval course of 96 h, including the controls (i.e. mock-transfected PC-3 cells) Lane 1: PC-3 control (24 h); lane 2: PC-3-LY2835218, LEE011, Palbociclib Treated, PC-3-hsa-miR-3202-pmR-ZsGreen1 DNA and PC-3-hsa-miR-7152-pmR-ZsGreen1 DNA (24 h); lane 3: PC-3-LY2835218, LEE011, Palbociclib Treated, PC-3-

hsa-miR-7152-pmR-ZsGreen1 DNA and PC-3-hsa-miR-7152-pmR-ZsGreen1 DNA (48 h); lane 4: PC-3-LY2835218, LEE011, Palbociclib Treated, PC-3-hsa-miR-3202-pmR-ZsGreen1 DNA and PC-3-hsa-miR-7152-pmR-ZsGreen1 DNA (96 h). **(B)** Bar Graph showing protein expression of CASP9 at different conditon expressions of LY2835219, LEE011, Palbociclib, hsa-miR-3202-pmR-ZsGreen1 and hsa-miR-7152-pmR-ZsGreen1 DNA with standard error bars and trimmed signal values.

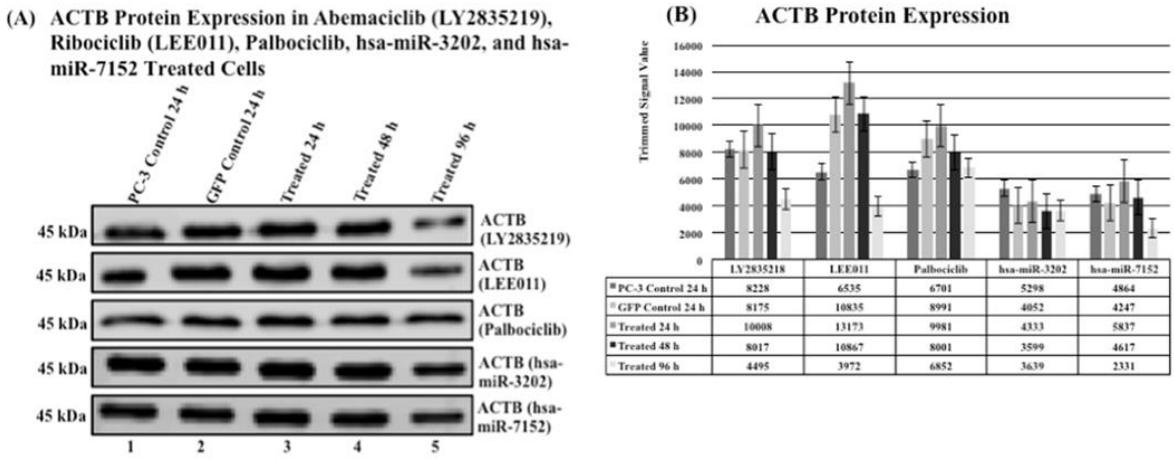

Figure 12: Western Blot and Bar Graph Analyses Comparisons of LY2835218, LEE001, Palbociclib, hsa-miR-3202-pmR-ZsGreen1 DNA and hsa-miR-7152-pmR-ZsGreen1 DNA on the Expression of ACTB

Figure 12: **(A)** Western blot protein expressions of ACTB in PC-3 cells that were treated with LY2835218, LEE001, Palbociclib and transient-transfected with pre-hsa-miR-3202-pmR-ZsGreen1 DNA and pre-hsa-miR-7152-pmR-ZsGreen1 DNA constructs in a 24 h interval course of 96 h, including the controls (i.e. mock-transfected PC-3 cells and pmR-ZsGreen1 vector DNA transient-transfected in PC-3 cells). Lane 1: PC-3 control (24

h); lane 2: PC-3-pmR-ZsGreen1vector DNA only (24 h); lane 3: PC-3-LY2835218, LEE011, Palbociclib Treated, PC-3-hsa-miR-3202-pmR-ZsGreen1 DNA and PC-3-hsa-miR-7152-pmR-ZsGreen1 DNA (24 h); lane 4: PC-3-LY2835218, LEE011, Palbociclib Treated, PC-3-hsa-miR-7152-pmR-ZsGreen1 DNA and PC-3-hsa-miR-7152-pmR-ZsGreen1 DNA (48 h); lane 5: PC-3-LY2835218, LEE011, Palbociclib Treated, PC-3-hsa-miR-3202-pmR-ZsGreen1 DNA and PC-3-hsa-miR-7152-pmR-ZsGreen1 DNA (96 h). **(B)** Bar Graph showing protein expression of ACTB at different conditon expressions of LY2835219, LEE011, Palbociclib, hsa-miR-3202-pmR-ZsGreen1 DNA and hsa-miR-7152-pmR-ZsGreen1 DNA with standard error bars and trimmed signal values.

Table 1: Statistical Analyses of LY2835218 and hsa-miR-3202-pmR-ZsGreen1 DNA on the Expression of CCND1

(Table 1A)

Analysis of Variance Results of CCND1
F-statistic value = 4.61014
P-value = 0.0983

Data Summary

Groups	N	Mean	Std. Dev.	Std. Error
LY2835218	3	0.0149	0.0225	0.013
hsa-miR-3202	3	0.3231	0.2476	0.143

(Table 1B)

ANOVA Summary					
Source	Degrees of Freedom	Sum of Squares	Mean Square	F-Stat	P-Value
	DF	SS	MS		
Between Groups	1	0.1425	0.1425	4.6101	0.0983
Within Groups	4	0.1236	0.0309		
Total:	5	0.2661			

Table 1A shows the variance results of CCND1 for each protein group pixel intensity signal values (i.e., the mean, standard deviation, and standard error) for LY2835218 and hsa-miR-3202-pmR-ZsGreen1 DNA as compared to the experimental control. **Table 1B** is the ANOVA Summary. It shows that when alpha equals .05 ($\alpha = .05$),

the p-value equals .0984 (p > .05), and the F statistic value equals 4.6071. The F-statistic is insignificant, showing there is a no spread out within the group means compared to the data variability within groups, demonstrating no differences between the group means.

Table 2: Statistical Analyses Comparisons of LY2835218, LEE001, Palbociclib and hsa-miR-7152-pmR-ZsGreen1 DNA on the Expression of CDK4

(Table 2A) **Analysis of Variance Results of CDK4**
F-statistic value = 2.23874
P-value = 0.16109

Data Summary

Groups	N	Mean	Std. Dev.	Std. Error
LY2835218	3	0.0307	0.0272	0.0157
LEE001	3	0.5385	0	0
Palbociclib	3	0.1795	0.3109	0.1795
hsa-miR-7152	3	0.6696	0.6185	0.3571

(Table 2B)

ANOVA Summary					
Source	Degrees of Freedom	Sum of Squares	Mean Square	F-Stat	P-Value
	DF	SS	MS		
Between Groups	3	0.8058	0.2686	2.2387	0.1611
Within Groups	8	0.9599	0.12		
Total:	11	1.7657			

Table 2A shows the variance results of CDK4 for each protein group pixel intensity signal values (i.e., the mean, standard deviation, and standard error) for LY2835218, LEE001, Palbociclib and hsa-miR-7152-pmR-ZsGreen1 DNA as compared to the experimental control. **Table 2B** is the ANOVA Summary. It shows that when alpha equals .05 ($\alpha = .05$), the p-value equals .1603 (p > .05), and the F statistic value equals 2.2451. The F-statistic is insignificant, showing there is a no spread out within the group means compared to the data variability within groups, demonstrating no differences between the group means.

Table 3: Statistical Analyses Comparisons of LY2835218, LEE001, Palbociclib, hsa-miR-3202-pmR-ZsGreen1 DNA and hsa-miR-7152-pmR-ZsGreen1 DNA on the Expression of AKT

(Table 3A) **Analysis of Variance Results of AKT**
F-statistic value = 7.44649
P-value = 0.00476

Data Summary

Groups	N	Mean	Std. Dev.	Std. Error
LY2835218	3	0.5417	0.4108	0.2372
LEE001	3	0.1637	0.12	0.0693
Palbociclib	3	0.2092	0.1396	0.0806
hsa-miR-3202	3	1.1617	0.489	0.2823
hsa-miR7152	3	1.216	0.2722	0.1571

(Table 3B)

ANOVA Summary					
Source	Degrees of Freedom	Sum of Squares	Mean Square	F-Stat	P-Value
	DF	SS	MS		
Between Groups	4	3.0731	0.7683	7.4465	0.0048
Within Groups	10	1.0317	0.1032		
Total:	14	4.1048			

Table 3A shows the variance results of AKT for each protein group pixel intensity signal values (i.e., the mean, standard deviation, and standard error) for LY2835218, LEE001, Palbociclib, hsa-miR-3202-pmR-ZsGreen1 DNA and hsa-miR-7152-pmR-ZsGreen1 DNA as compared to the experimental control. **Table 3B** is the ANOVA Summary. It shows that when alpha equals .05 ($\alpha = .05$), the p-value equals .0048 ($p < .05$), and the F statistic value equals 7.4473. The F-statistic is significant, showing there is a spread out within the group means compared to the data variability within groups, demonstrating the differences between the group means.

Table 4: Statistical Analyses Comparisons of LY2835218, LEE001, Palbociclib, hsa-miR-3202-pmR-ZsGreen1 DNA and hsa-miR-7152-pmR-ZsGreen1 DNA on the Expression of Bcl-xL

(Table 4A) Analysis of Variance Results of Bcl-xL
F-statistic value = 1.27031
P-value = 0.34411

Data Summary

Groups	N	Mean	Std. Dev.	Std. Error
LY2835218	3	0.4464	0.2498	0.1442
LEE001	3	0.455	0.0425	0.0245
Palbociclib	3	1.332	1.8388	1.0616
hsa-miR-3202	3	1.0619	0.1006	0.0581
hsa-miR7152	3	1.7953	0.7246	0.4184

(Table 4B)

ANOVA Summary					
Source	Degrees of Freedom	Sum of Squares	Mean Square	F-Stat	P-Value
	DF	SS	MS		
Between Groups	4	4.0452	1.0113	1.2703	0.3441
Within Groups	10	7.9611	0.7961		
Total:	14	12.0064			

Table 4A shows the variance results of Bcl-xL for each protein group pixel intensity signal values (i.e., the mean, standard deviation, and standard error) for LY2835218, LEE001, Palbociclib, hsa-miR-3202-pmR-ZsGreen1 DNA and hsa-miR-7152-pmR-ZsGreen1 DNA as compared to the experimental control. **Table 4B** is the ANOVA Summary. It shows that when alpha equals .05 ($\alpha = .05$), the p-value equals .3441 ($p > .05$), and the F statistic value equals 1.2703. The F-statistic is insignificant, showing there is a no spread out within the group means compared to the data variability within groups, demonstrating no differences between the group means.

Table 5: Statistical Analyses Comparisons of LY2835218, LEE001, Palbociclib, hsa-miR-3202-pmR-ZsGreen1 DNA and hsa-miR-7152-pmR-ZsGreen1 DNA on the Expression of CASP9

(Table 5A) **Analysis of Variance Results of CASP9**
F-statistic value = 0.823
P-value = 0.53948

Data Summary

Groups	N	Mean	Std. Dev.	Std. Error
LY2835218	3	0.1487	0.1404	0.0811
LEE001	3	0.94	1.0871	0.6276
Palbociclib	3	0.3725	0.5466	0.3156
hsa-miR-3202	3	0.3637	0.2653	0.1532
hsa-miR7152	3	0.6067	0.2831	0.1634

(Table 5B)

ANOVA Summary					
Source	Degrees of Freedom	Sum of Squares	Mean Square	F-Stat	P-Value
	DF	SS	MS		
Between Groups	4	1.0869	0.2717	0.823	0.5395
Within Groups	10	3.3016	0.3302		
Total:	14	4.3885			

Table 5A shows the variance results of CASP9 for each protein group pixel intensity signal values (i.e., the mean, standard deviation, and standard error) for LY2835218, LEE001, Palbociclib, hsa-miR-3202-pmR-ZsGreen1 DNA and hsa-miR-7152-pmR-ZsGreen1 DNA as compared to the experimental control. **Table 5B**, the ANOVA Summary, shows, that when alpha equals .05 ($\alpha = .05$), the p-value equals .5351 ($p > .05$), and the F statistic value equals 0.8311. The F-statistic is insignificant, showing there is a no spread out within the group means compared to the data variability within groups, demonstrating no differences between the group means.

Table 6: Statistical Analyses Comparisons of LY2835218, LEE001, Palbociclib, hsa-miR-3202-pmR-ZsGreen1 DNA and hsa-miR-7152-pmR-ZsGreen1 DNA on the Expression of ACTB

(Table 6A) **Analysis of Variance Results of ACTB**
F-statistic value = 3.51491
P-value = 0.03247

Data Summary

Groups	N	Mean	Std. Dev.	Std. Error
LY2835218	4	0.9326	0.28	0.14
LEE001	4	1.4861	0.609	0.3045
Palbociclib	4	1.3048	0.1414	0.0707
hsa-miR-3202	4	0.7372	0.0662	0.0331
hsa-miR7152	4	0.8754	0.2988	0.1494

(Table 6B)

ANOVA Summary					
Source	Degrees of Freedom	Sum of Squares	Mean Square	F-Stat	P-Value
	DF	SS	MS		
Between Groups	4	1.5829	0.3957	3.5149	0.0325
Within Groups	15	1.6888	0.1126		
Total:	19	3.2718			

Table 6A shows the variance results of ACTB for each protein group pixel intensity signal values (i.e., the mean, standard deviation, and standard error) for LY2835218, LEE001, Palbociclib, hsa-miR-3202-pmR-ZsGreen1 DNA and hsa-miR-7152-pmR-ZsGreen1 DNA as compared to the experimental controls. **Table 6B,** the ANOVA Summary shows, that when alpha equals .05 ($\alpha = .05$), the p-value equals .0325 ($p < .05$), and the F statistic value equals 3.5149. The F-statistic is significant, showing there is a spread out within the group means compared to the data variability within groups, demonstrating the differences between the group means

CHAPTER 5

SUMMARY, CONCLUSIONS, AND RECOMMENDATIONS

This study demonstrated that the comparison between both the xenobiotic drugs (LY2835218, LEE001, and Palbociclib) and miRs (hsa-miR-3202 and hsa-miR-7152) would influence the protein of the cell cycle and apoptotic regulators in PC-3 cells. The results characterized that the xenobiotic drugs are more potent than the miRNAs since they directly interact with the protein they inhibit. Abemaciclib (LY2835219) completely inhibits CCND1 and CDK4 protein expression at every interval hour in PC-3 cells. Ribociclib (LEE011) and Palbociclib also completely inhibit CDK4 protein expression at every interval, except subtle CDK4 protein expression was observed at 24 h. However, Palbociclib inhibits CDK4 more at 48 h and 96 h than at 24 h. hsa-miR-3202 reduces CCND1 protein expression at 48 h and 96 h but is not as potent as the xenobiotic drugs that directly interact with the proteins. hsa-miR-7152 reduced CDK4 protein expression at 48 h, but it was more potent at 96 h. Yet the xenobiotic drugs are far more powerful. The xenobiotic drugs ultimately inhibit AKT and CASP9 protein expression at 96 h, and at 48 h, the two proteins' expressions were low, suggesting that they affect proteins in the AKT pathway. Yet miRNA’s effect on AKT protein expression is subtle. The miRNAs reduce CASP9 protein expression at 96 h. The xenobiotic drugs also reduce Bcl-xL protein expression at 48 h and 96 h, but the miRNAs effect on Bcl-xL protein expression is subtle. Only Abemaciclib (LY2835219) and Ribociclib (LEE011) slightly reduce ACTB protein expression.

Finally, the overall findings of this study suggest that This is the first report that compared and showed that overexpression miRs are less potent than xenobiotic drugs that directly interact with their target proteins. The result suggests that miRNA tested in the study as compared to the drugs may be less harmful or toxic to cells. Yet other miRNAs may be more potent, especially those miRNAs that function as tumor suppressors or oncogenes. The results also show that genes in the AKT pathway, which is upstream of our target genes, are also affected by the miRNA and the xenobiotic drugs to a certain extent in PC-3 cells.

REFERENCES

Ameratunga, M., Kipps, E., Okines, A. F. C., & Lopez, J. S. (2019). To Cycle or Fight-CDK4/6 Inhibitors at the Crossroads of Anticancer Immunity. Clin Cancer Res, 25(1), 21-28. doi: 10.1158/1078-0432.CCR-18-1999 PMID: 30224338

Anders, L., Ke, N., Hydbring, P., Choi, Y. J., Widlund, H. R., Chick, J. M., . . . Sicinski, P. (2011). A systematic screen for CDK4/6 substrates links FOXM1 phosphorylation to senescence suppression in cancer cells. Cancer Cell, 20(5), 620-634. doi: 10.1016/j.ccr.2011.10.001 PMCID: PMC3237683

Arboleda, M. J., Lyons, J. F., Kabbinavar, F. F., Bray, M. R., Snow, B. E., Ayala, R., . . . Slamon, D. J. (2003). Overexpression of AKT2/protein kinase Bbeta leads to up-regulation of beta1 integrins, increased invasion, and metastasis of human breast and ovarian cancer cells. Cancer Res, 63(1), 196-206. PMID: 12517798

Arcaro, A., & Guerreiro, A. S. (2007). The phosphoinositide 3-kinase pathway in human cancer: genetic alterations and therapeutic implications. Curr Genomics, 8(5), 271-306. doi: 10.2174/138920207782446160 PMID: 19384426

Asghar, U., Witkiewicz, A. K., Turner, N. C., & Knudsen, E. S. (2015). The history and future of targeting cyclin-dependent kinases in cancer therapy. Nat Rev Drug Discov, 14(2), 130-146. doi: 10.1038/nrd4504 PMID: 25633797

Babiarz, J. E., Ruby, J. G., Wang, Y., Bartel, D. P., & Blelloch, R. (2008). Mouse ES cells express endogenous shRNAs, siRNAs, and other Microprocessor-independent, Dicer-dependent small RNAs. Genes Dev, 22(20), 2773-2785. doi: 10.1101/gad.1705308 PMID: 18923076.

Bagui, T. K., Mohapatra, S., Haura, E., & Pledger, W. J. (2003). P27Kip1 and p21Cip1 are not required for the formation of active D cyclin-cdk4 complexes. Mol Cell Biol, 23(20), 7285-7290. doi: 10.1128/MCB.23.20.7285-7290.2003 PMID: 14517297

Bardia A, et al. Phase Ib/II study of LEE011, everolimus, and exemestane in postmenopausal women with ER+/HER2-metastatic breast cancer. J Clin Oncol 2014; 32: 535–535.

Bardia A, et al. Triplet therapy with ribociclib, everolimus, and exemestane in women with HR+/HER2– advanced breast cancer. In: San Antonio Breast Cancer Symposium, 8–12 December 2015, Springer Healthcare Limited: San Antonio, Texas. p.1436.

Barnett, S. F., Defeo-Jones, D., Fu, S., Hancock, P. J., Haskell, K. M., Jones, R. E., . . . Huber, H. E. (2005). Identification and characterization of pleckstrin-homology-domain-dependent and isoenzyme-specific Akt inhibitors. Biochem J, 385(Pt 2), 399-408. doi: 10.1042/BJ20041140 PMID: 15456405

Baughn, L. B., Di Liberto, M., Wu, K., Toogood, P. L., Louie, T., Gottschalk, R., . . . Chen-Kiang, S. (2006). A novel orally active small molecule potently induces G1 arrest in primary myeloma cells and prevents tumor growth by specific inhibition

of cyclin-dependent kinase 4/6. Cancer Res, 66(15), 7661-7667. doi: 10.1158/0008-5472.CAN-06-1098 PMID: 16885367

Bhutani, J., Sheikh, A., & Niazi, A. K. (2013). Akt inhibitors: mechanism of action and implications for anticancer therapeutics. Infect Agent Cancer, 8(1), 49. doi: 10.1186/1750-9378-8-49 PMID: 24330834

Blain, S. W. (2008). Switching cyclin D-Cdk4 kinase activity on and off. Cell Cycle, 7(7), 892-898. doi: 10.4161/cc.7.7.5637 PMID: 18414028

Blain, S. W., Montalvo, E., & Massague, J. (1997). Differential interaction of the cyclin-dependent kinase (Cdk) inhibitor p27Kip1 with cyclin A-Cdk2 and cyclin D2-Cdk4. J Biol Chem, 272(41), 25863-25872. doi: 10.1074/jbc.272.41.25863 PMID: 9325318

Bratton, S. B., & Salvesen, G. S. (2010). Regulation of the Apaf-1-caspase-9 apoptosome. J Cell Sci, 123(Pt 19), 3209-3214. doi: 10.1242/jcs.073643 PMID: 20844150

Bunnell, T. M., Burbach, B. J., Shimizu, Y., & Ervasti, J. M. (2011). beta-Actin specifically controls cell growth, migration, and the G-actin pool. Mol Biol Cell, 22(21), 4047-4058. doi: 10.1091/mbc.E11-06-0582 PMID: 21900491

Burke T, Torres R, McNulty A, et al. The major human metabolites of abemaciclib are inhibitors of CDK4 and CDK6 [abstract 2830]. Abstract presented at: 107th Annual Meeting of the American Association for Cancer Research; April 16-20, 2016; New Orleans, LA.

Canepa, E. T., Scassa, M. E., Ceruti, J. M., Marazita, M. C., Carcagno, A. L., Sirkin, P. F., & Ogara, M. F. (2007). INK4 proteins, a family of mammalian CDK inhibitors

with novel biological functions. IUBMB Life, 59(7), 419-426. doi: 10.1080/15216540701488358 PMID: 17654117

Carmona, F. J., Montemurro, F., Kannan, S., Rossi, V., Verma, C., Baselga, J., & Scaltriti, M. (2016). AKT signaling in ERBB2-amplified breast cancer. Pharmacol Ther, 158, 63-70. doi: 10.1016/j.pharmthera.2015.11.013 PMID: 26645663

Carpten, J. D., Faber, A. L., Horn, C., Donoho, G. P., Briggs, S. L., Robbins, C. M., . . . Thomas, J. E. (2007). A transforming mutation in the pleckstrin homology domain of AKT1 in cancer. Nature, 448(7152), 439-444. doi: 10.1038/nature05933 PMID: 17611497

Castilla-Llorente, V., Spraggon, L., Okamura, M., Naseeruddin, S., Adamow, M., Qamar, S., & Liu, J. (2012). Mammalian GW220/TNGW1 is essential for the formation of GW/P bodies containing miRISC. J Cell Biol, 198(4), 529-544. doi: 10.1083/jcb.201201153 PMID: 22891262

Chan, J. A., Krichevsky, A. M., & Kosik, K. S. (2005). MicroRNA-21 is an antiapoptotic factor in human glioblastoma cells. Cancer Res, 65(14), 6029-6033. doi: 10.1158/0008-5472.CAN-05-0137 PMID: 16024602

Chen, P., Lee, N. V., Hu, W., Xu, M., Ferre, R. A., Lam, H., . . . Murray, B. W. (2016). Spectrum and Degree of CDK Drug Interactions Predicts Clinical Performance. Mol Cancer Ther, 15(10), 2273-2281. doi: 10.1158/1535-7163.MCT-16-0300 PMID: 27496135

Chen, Y., Zhu, X., Zhang, X., Liu, B., & Huang, L. (2010). Nanoparticles modified with tumor-targeting scFv deliver siRNA and miRNA for cancer therapy. Mol Ther, 18(9), 1650-1656. doi: 10.1038/mt.2010.136 PMID: 20606648

Chendrimada, T. P., Gregory, R. I., Kumaraswamy, E., Norman, J., Cooch, N., Nishikura, K., & Shiekhattar, R. (2005). TRBP recruits the Dicer complex to Ago2 for microRNA processing and gene silencing. Nature, 436(7051), 740-744. doi: 10.1038/nature03868 PMID: 15973356

Cheon, D. J., & Orsulic, S. (2011). Mouse models of cancer. Annu Rev Pathol, 6, 95-119. doi: 10.1146/annurev.pathol.3.121806.154244 PMID: 20936938

Chipuk, J. E., Kuwana, T., Bouchier-Hayes, L., Droin, N. M., Newmeyer, D. D., Schuler, M., & Green, D. R. (2004). Direct activation of Bax by p53 mediates mitochondrial membrane permeabilization and apoptosis. Science, 303(5660), 1010-1014. doi: 10.1126/science.1092734 PMID: 14963330

Chipuk, J. E., Bouchier-Hayes, L., Kuwana, T., Newmeyer, D. D., & Green, D. R. (2005). PUMA couples the nuclear and cytoplasmic proapoptotic function of p53. Science, 309(5741), 1732-1735. doi: 10.1126/science.1114297 PMID: 16151013

Ciafre, S. A., Galardi, S., Mangiola, A., Ferracin, M., Liu, C. G., Sabatino, G., . . . Farace, M. G. (2005). Extensive modulation of a set of microRNAs in primary glioblastoma. Biochem Biophys Res Commun, 334(4), 1351-1358. doi: 10.1016/j.bbrc.2005.07.030 PMID: 16039986

Cleary, M. L., Smith, S. D., & Sklar, J. (1986). Cloning and structural analysis of cDNAs for bcl-2 and a hybrid bcl-2/immunoglobulin transcript resulting from the t(14;18)

translocation. Cell, 47(1), 19-28. doi: 10.1016/0092-8674(86)90362-4 PMID: 2875799

Connell-Crowley, L., Harper, J. W., & Goodrich, D. W. (1997). Cyclin D1/Cdk4 regulates retinoblastoma protein-mediated cell cycle arrest by site-specific phosphorylation. Mol Biol Cell, 8(2), 287-301. doi: 10.1091/mbc.8.2.287 PMID: 9190208

Cristiano, B. E., Chan, J. C., Hannan, K. M., Lundie, N. A., Marmy-Conus, N. J., Campbell, I. G., . . . Pearson, R. B. (2006). A specific role for AKT3 in the genesis of ovarian cancer through modulation of G(2)-M phase transition. Cancer Res, 66(24), 11718-11725. doi: 10.1158/0008-5472.CAN-06-1968 PMID: 17178867

Czabotar, P. E., Lessene, G., Strasser, A., & Adams, J. M. (2014). Control of apoptosis by the BCL-2 protein family: implications for physiology and therapy. Nat Rev Mol Cell Biol, 15(1), 49-63. doi: 10.1038/nrm3722 PMID: 24355989

Czech, B., Zhou, R., Erlich, Y., Brennecke, J., Binari, R., Villalta, C., . . . Hannon, G. J. (2009). Hierarchical rules for Argonaute loading in Drosophila. Mol Cell, 36(3), 445-456. doi: 10.1016/j.molcel.2009.09.028 PMID: 19917252

Denli, A. M., Tops, B. B., Plasterk, R. H., Ketting, R. F., & Hannon, G. J. (2004). Processing of primary microRNAs by the Microprocessor complex. Nature, 432(7014), 231-235. doi: 10.1038/nature03049 PMID: 15531879

Denicourt, C., & Dowdy, S. F. (2004). Cip/Kip proteins: more than just CDKs inhibitors. Genes Dev, 18(8), 851-855. doi: 10.1101/gad.1205304 PMID: 15107401

Di Leva G, Gasparini P, Piovan C: A regulatory “miRcircuitry” involving miR-221&222 and ER determines ERα status of breast cancer cells. J Natl Cancer Inst (in press)

Dickler, M., Tolaney, S., Rugo, H., Cortes, J., Diéras, V., Patt, D., Wildiers, H., Frenzel, M., Koustenis, A. and Baselga, J. (2016). MONARCH1: Results from a phase II study of abemaciclib, a CDK4 and CDK6 inhibitor, as monotherapy, in patients with HR+/HER2- breast cancer, after chemotherapy for advanced disease. Journal of Clinical Oncology, 34(15_suppl), pp.510-510.

Downward, J. (2004). PI 3-kinase, Akt and cell survival. Semin Cell Dev Biol, 15(2), 177-182. doi: 10.1016/j.semcdb.2004.01.002 PMID: 15209377

D'Sa-Eipper, C., Leonard, J. R., Putcha, G., Zheng, T. S., Flavell, R. A., Rakic, P., . . . Roth, K. A. (2001). DNA damage-induced neural precursor cell apoptosis requires p53 and caspase 9 but neither Bax nor caspase 3. Development, 128(1), 137-146. doi: 10.1242/dev.128.1.137 PMID: 11092819

Dummler, B., & Hemmings, B. A. (2007). Physiological roles of PKB/Akt isoforms in development and disease. Biochem Soc Trans, 35(Pt 2), 231-235. doi: 10.1042/BST0350231 PMID: 17371246

Easton, R. M., Cho, H., Roovers, K., Shineman, D. W., Mizrahi, M., Forman, M. S., . . . Birnbaum, M. J. (2005). Role for Akt3/protein kinase Bgamma in attainment of normal brain size. Mol Cell Biol, 25(5), 1869-1878. doi: 10.1128/MCB.25.5.1869-1878.2005 PMID: 15713641

Ender, C., Krek, A., Friedlander, M. R., Beitzinger, M., Weinmann, L., Chen, W., . . . Meister, G. (2008). A human snoRNA with microRNA-like functions. Mol Cell, 32(4), 519-528. doi: 10.1016/j.molcel.2008.10.017 PMID: 19026782

Finn, R. S., Crown, J. P., Lang, I., Boer, K., Bondarenko, I. M., Kulyk, S. O., . . . Slamon, D. J. (2015). The cyclin-dependent kinase 4/6 inhibitor palbociclib in combination with letrozole versus letrozole alone as first-line treatment of oestrogen receptor-positive, HER2-negative, advanced breast cancer (PALOMA-1/TRIO-18): a randomised phase 2 study. Lancet Oncol, 16(1), 25-35. doi: 10.1016/S1470-2045(14)71159-3 PMID: 25524798

Finn, R. S., Martin, M., Rugo, H. S., Jones, S., Im, S. A., Gelmon, K., . . . Slamon, D. J. (2016). Palbociclib and Letrozole in Advanced Breast Cancer. N Engl J Med, 375(20), 1925-1936. doi: 10.1056/NEJMoa1607303 PMID: 27959613

Fry, D. W., Harvey, P. J., Keller, P. R., Elliott, W. L., Meade, M., Trachet, E., . . . Toogood, P. L. (2004). Specific inhibition of cyclin-dependent kinase 4/6 by PD 0332991 and associated antitumor activity in human tumor xenografts. Mol Cancer Ther, 3(11), 1427-1438. PMID: 15542782

Fu, L. Y., Jia, H. L., Dong, Q. Z., Wu, J. C., Zhao, Y., Zhou, H. J., . . . Qin, L. X. (2009). Suitable reference genes for real-time PCR in human HBV-related hepatocellular carcinoma with different clinical prognoses. BMC Cancer, 9, 49. doi: 10.1186/1471-2407-9-49 PMID: 19200351

Gabellini, C., Trisciuoglio, D., & Del Bufalo, D. (2017). Non-canonical roles of Bcl-2 and Bcl-xL proteins: relevance of BH4 domain. Carcinogenesis, 38(6), 579-587. doi: 10.1093/carcin/bgx016 PMID: 28203756

Gangwar, R., Mandhani, A., & Mittal, R. D. (2009). Caspase 9 and caspase 8 gene polymorphisms and susceptibility to bladder cancer in north Indian population. Ann Surg Oncol, 16(7), 2028-2034. doi: 10.1245/s10434-009-0488-3 PMID: 19412632

Gelbert, L. M., Cai, S., Lin, X., Sanchez-Martinez, C., Del Prado, M., Lallena, M. J., . . . de Dios, A. (2014). Preclinical characterization of the CDK4/6 inhibitor LY2835219: in-vivo cell cycle-dependent/independent anti-tumor activities alone/in combination with gemcitabine. Invest New Drugs, 32(5), 825-837. doi: 10.1007/s10637-014-0120-7 PMID: 24919854

Geoerger, B., Bourdeaut, F., DuBois, S. G., Fischer, M., Geller, J. I., Gottardo, N. G., . . . Chi, S. N. (2017). A Phase I Study of the CDK4/6 Inhibitor Ribociclib (LEE011) in Pediatric Patients with Malignant Rhabdoid Tumors, Neuroblastoma, and Other Solid Tumors. Clin Cancer Res, 23(10), 2433-2441. doi: 10.1158/1078-0432.CCR-16-2898 PMID: 28432176

Gil, J., & Peters, G. (2006). Regulation of the INK4b-ARF-INK4a tumour suppressor locus: all for one or one for all. Nat Rev Mol Cell Biol, 7(9), 667-677. doi: 10.1038/nrm1987 PMID: 16921403

Goidin, D., Mamessier, A., Staquet, M. J., Schmitt, D., & Berthier-Vergnes, O. (2001). Ribosomal 18S RNA prevails over glyceraldehyde-3-phosphate dehydrogenase and beta-actin genes as internal standard for quantitative comparison of mRNA levels in invasive and noninvasive human melanoma cell subpopulations. Anal Biochem, 295(1), 17-21. doi: 10.1006/abio.2001.5171 PMID: 11476540

Grana, X., & Reddy, E. P. (1995). Cell cycle control in mammalian cells: role of cyclins, cyclin dependent kinases (CDKs), growth suppressor genes and cyclin-dependent kinase inhibitors (CKIs). Oncogene, 11(2), 211-219. PMID: 7624138

Grafstrom, R. H., Pan, W., & Hoess, R. H. (1999). Defining the substrate specificity of cdk4 kinase-cyclin D1 complex. Carcinogenesis, 20(2), 193-198. doi: 10.1093/carcin/20.2.193 PMID: 10069453

Gregory, R. I., Yan, K. P., Amuthan, G., Chendrimada, T., Doratotaj, B., Cooch, N., & Shiekhattar, R. (2004). The Microprocessor complex mediates the genesis of microRNAs. Nature, 432(7014), 235-240. doi: 10.1038/nature03120 PMID: 15531877

Hakem, R., Hakem, A., Duncan, G. S., Henderson, J. T., Woo, M., Soengas, M. S., . . . Mak, T. W. (1998). Differential requirement for caspase 9 in apoptotic pathways in vivo. Cell, 94(3), 339-352. doi: 10.1016/s0092-8674(00)81477-4 PMID: 9708736

Han, J., Lee, Y., Yeom, K. H., Kim, Y. K., Jin, H., & Kim, V. N. (2004). The Drosha-DGCR8 complex in primary microRNA processing. Genes Dev, 18(24), 3016-3027. doi: 10.1101/gad.1262504 PMID: 15574589

Hanada, M., Feng, J., & Hemmings, B. A. (2004). Structure, regulation and function of PKB/AKT--a major therapeutic target. Biochim Biophys Acta, 1697(1-2), 3-16. doi: 10.1016/j.bbapap.2003.11.009 PMID: 15023346

Inaba, T., Matsushime, H., Valentine, M., Roussel, M. F., Sherr, C. J., & Look, A. T. (1992). Genomic organization, chromosomal localization, and independent

expression of human cyclin D genes. Genomics, 13(3), 565-574. doi: 10.1016/0888-7543(92)90126-d PMID: 1386335

Infante, J. R., Cassier, P. A., Gerecitano, J. F., Witteveen, P. O., Chugh, R., Ribrag, V., . . . Shapiro, G. I. (2016). A Phase I Study of the Cyclin-Dependent Kinase 4/6 Inhibitor Ribociclib (LEE011) in Patients with Advanced Solid Tumors and Lymphomas. Clin Cancer Res, 22(23), 5696-5705. doi: 10.1158/1078-0432.CCR-16-1248 PMID: 27542767

Iorio, M. V., Ferracin, M., Liu, C. G., Veronese, A., Spizzo, R., Sabbioni, S., . . . Croce, C. M. (2005). MicroRNA gene expression deregulation in human breast cancer. Cancer Res, 65(16), 7065-7070. doi: 10.1158/0008-5472.CAN-05-1783 PMID: 16103053

Iorio, M. V., Visone, R., Di Leva, G., Donati, V., Petrocca, F., Casalini, P., . . . Croce, C. M. (2007). MicroRNA signatures in human ovarian cancer. Cancer Res, 67(18), 8699-8707. doi: 10.1158/0008-5472.CAN-07-1936 PMID: 17875710

James, M. K., Ray, A., Leznova, D., & Blain, S. W. (2008). Differential modification of p27Kip1 controls its cyclin D-cdk4 inhibitory activity. Mol Cell Biol, 28(1), 498-510. doi: 10.1128/MCB.02171-06 PMID: 17908796

Johnson, S. M., Grosshans, H., Shingara, J., Byrom, M., Jarvis, R., Cheng, A., . . . Slack, F. J. (2005). RAS is regulated by the let-7 microRNA family. Cell, 120(5), 635-647. doi: 10.1016/j.cell.2005.01.014 PMID: 15766527

Kato, J., Matsushime, H., Hiebert, S. W., Ewen, M. E., & Sherr, C. J. (1993). Direct binding of cyclin D to the retinoblastoma gene product (pRb) and pRb

phosphorylation by the cyclin D-dependent kinase CDK4. Genes Dev, 7(3), 331-342. doi: 10.1101/gad.7.3.331 PMID: 8449399

Kato, J. Y., Matsuoka, M., Strom, D. K., & Sherr, C. J. (1994). Regulation of cyclin D-dependent kinase 4 (cdk4) by cdk4-activating kinase. Mol Cell Biol, 14(4), 2713-2721. doi: 10.1128/mcb.14.4.2713-2721.1994 PMID: 8139570

Kiechle, T., Dedeoglu, A., Kubilus, J., Kowall, N. W., Beal, M. F., Friedlander, R. M., . . . Ferrante, R. J. (2002). Cytochrome C and caspase-9 expression in Huntington's disease. Neuromolecular Med, 1(3), 183-195. doi: 10.1385/NMM:1:3:183 PMID: 12095160

Kim S, Loo A, Chopra R, et al. LEE011: an orally bioavailable, selective small molecule inhibitor of CDK4/6–Reactivating Rb in cancer. Mol Cancer Ther 2013;12: Suppl 11:PR02-PR02. Abstract

Kitagawa, M., Higashi, H., Jung, H. K., Suzuki-Takahashi, I., Ikeda, M., Tamai, K., . . . Taya, Y. (1996). The consensus motif for phosphorylation by cyclin D1-Cdk4 is different from that for phosphorylation by cyclin A/E-Cdk2. EMBO J, 15(24), 7060-7069. PMID: 9003781

Klein, M. E., Kovatcheva, M., Davis, L. E., Tap, W. D., & Koff, A. (2018). CDK4/6 Inhibitors: The Mechanism of Action May Not Be as Simple as Once Thought. Cancer Cell, 34(1), 9-20. doi: 10.1016/j.ccell.2018.03.023 PMID: 29731395

Kroeger, P. T., Jr., & Drapkin, R. (2017). Pathogenesis and heterogeneity of ovarian cancer. Curr Opin Obstet Gynecol, 29(1), 26-34. doi: 10.1097/GCO.0000000000000340 PMID: 27898521

Kuida, K., Haydar, T. F., Kuan, C. Y., Gu, Y., Taya, C., Karasuyama, H., . . . Flavell, R. A. (1998). Reduced apoptosis and cytochrome c-mediated caspase activation in mice lacking caspase 9. Cell, 94(3), 325-337. doi: 10.1016/s0092-8674(00)81476-2 PMID: 9708735

Kumar, M. S., Erkeland, S. J., Pester, R. E., Chen, C. Y., Ebert, M. S., Sharp, P. A., & Jacks, T. (2008). Suppression of non-small cell lung tumor development by the let-7 microRNA family. Proc Natl Acad Sci U S A, 105(10), 3903-3908. doi: 10.1073/pnas.0712321105 PMID: 18308936

Kuwahara, D., Tsutsumi, K., Oyake, D., Ohta, T., Nishikawa, H., & Koizuka, I. (2003). Inhibition of caspase-9 activity and Apaf-1 expression in cisplatin-resistant head and neck squamous cell carcinoma cells. Auris Nasus Larynx, 30 Suppl, S85-88. doi: 10.1016/s0385-8146(02)00129-3 PMID: 12543167

Lagos-Quintana, M., Rauhut, R., Meyer, J., Borkhardt, A., & Tuschl, T. (2003). New microRNAs from mouse and human. RNA, 9(2), 175-179. doi: 10.1261/rna.2146903 PMID: 12554859

Lallena, M., Boehnke, K., Torres, R., Hermoso, A., Amat, J., Calsina, B., De Dios, A., Buchanan, S., Du, J., Beckmann, R., Gong, X. and Mcnulty, A. (2015). Abstract 3101: In-vitro characterization of Abemaciclib pharmacology in ER+ breast cancer cell lines. Molecular and Cellular Biology.

Landthaler, M., Yalcin, A., & Tuschl, T. (2004). The human DiGeorge syndrome critical region gene 8 and Its D. melanogaster homolog are required for miRNA biogenesis. Curr Biol, 14(23), 2162-2167. doi: 10.1016/j.cub.2004.11.001 PMID: 15589161

Larochelle, S., Pandur, J., Fisher, R. P., Salz, H. K., & Suter, B. (1998). Cdk7 is essential for mitosis and for in vivo Cdk-activating kinase activity. Genes Dev, 12(3), 370-381. doi: 10.1101/gad.12.3.370 PMID: 9450931

Larrea, M. D., Liang, J., Da Silva, T., Hong, F., Shao, S. H., Han, K., . . . Slingerland, J. M. (2008). Phosphorylation of p27Kip1 regulates assembly and activation of cyclin D1-Cdk4. Mol Cell Biol, 28(20), 6462-6472. doi: 10.1128/MCB.02300-07 PMID: 18710949

Lau, N. C., Lim, L. P., Weinstein, E. G., & Bartel, D. P. (2001). An abundant class of tiny RNAs with probable regulatory roles in Caenorhabditis elegans. Science, 294(5543), 858-862. doi: 10.1126/science.1065062 PMID: 11679671

Le, P. U., Nguyen, T. N., Drolet-Savoie, P., Leclerc, N., & Nabi, I. R. (1998). Increased beta-actin expression in an invasive moloney sarcoma virus-transformed MDCK cell variant concentrates to the tips of multiple pseudopodia. Cancer Res, 58(8), 1631-1635. PMID: 9563473

Lee, Y., Ahn, C., Han, J., Choi, H., Kim, J., Yim, J., . . . Kim, V. N. (2003). The nuclear RNase III Drosha initiates microRNA processing. Nature, 425(6956), 415-419. doi: 10.1038/nature01957 PMID: 14508493

Lee, R. C., Feinbaum, R. L., & Ambros, V. (1993). The C. elegans heterochronic gene lin-4 encodes small RNAs with antisense complementarity to lin-14. Cell, 75(5), 843-854. doi: 10.1016/0092-8674(93)90529-y PMID: 8252621

Lee, Y., Hur, I., Park, S. Y., Kim, Y. K., Suh, M. R., & Kim, V. N. (2006). The role of PACT in the RNA silencing pathway. EMBO J, 25(3), 522-532. doi: 10.1038/sj.emboj.7600942 PMID: 16424907

Lee, Y., Jeon, K., Lee, J. T., Kim, S., & Kim, V. N. (2002). MicroRNA maturation: stepwise processing and subcellular localization. EMBO J, 21(17), 4663-4670. doi: 10.1093/emboj/cdf476 PMID: 12198168

Leonard, J. P., LaCasce, A. S., Smith, M. R., Noy, A., Chirieac, L. R., Rodig, S. J., . . . Shapiro, G. I. (2012). Selective CDK4/6 inhibition with tumor responses by PD0332991 in patients with mantle cell lymphoma. Blood, 119(20), 4597-4607. doi: 10.1182/blood-2011-10-388298 PMID: 22383795

Liamarkopoulos, E., Gazouli, M., Aravantinos, G., Tzanakis, N., Theodoropoulos, G., Rizos, S., & Nikiteas, N. (2011). Caspase 8 and caspase 9 gene polymorphisms and susceptibility to gastric cancer. Gastric Cancer, 14(4), 317-321. doi: 10.1007/s10120-011-0045-1 PMID: 21461653

Li, J., Poi, M. J., & Tsai, M. D. (2011). Regulatory mechanisms of tumor suppressor P16(INK4A) and their relevance to cancer. Biochemistry, 50(25), 5566-5582. doi: 10.1021/bi200642e PMID: 21619050

Li, P., Nijhawan, D., Budihardjo, I., Srinivasula, S. M., Ahmad, M., Alnemri, E. S., & Wang, X. (1997). Cytochrome c and dATP-dependent formation of Apaf-1/caspase-9 complex initiates an apoptotic protease cascade. Cell, 91(4), 479-489. doi: 10.1016/s0092-8674(00)80434-1 PMID: 9390557

Li, W., Xie, L., He, X., Li, J., Tu, K., Wei, L., . . . Gu, J. (2008). Diagnostic and prognostic implications of microRNAs in human hepatocellular carcinoma. Int J Cancer, 123(7), 1616-1622. doi: 10.1002/ijc.23693 PMID: 18649363

Longmire, M., Choyke, P. L., & Kobayashi, H. (2008). Clearance properties of nano-sized particles and molecules as imaging agents: considerations and caveats. Nanomedicine (Lond), 3(5), 703-717. doi: 10.2217/17435889.3.5.703 PMID: 18817471

Lund, E., Guttinger, S., Calado, A., Dahlberg, J. E., & Kutay, U. (2004). Nuclear export of microRNA precursors. Science, 303(5654), 95-98. doi: 10.1126/science.1090599 PMID: 14631048

Lundberg, A. S., & Weinberg, R. A. (1998). Functional inactivation of the retinoblastoma protein requires sequential modification by at least two distinct cyclin-cdk complexes. Mol Cell Biol, 18(2), 753-761. doi: 10.1128/MCB.18.2.753 PMID: 9447971

Lv, H., Zhang, S., Wang, B., Cui, S., & Yan, J. (2006). Toxicity of cationic lipids and cationic polymers in gene delivery. J Control Release, 114(1), 100-109. doi: 10.1016/j.jconrel.2006.04.014 PMID: 16831482

Mahony, D., Parry, D. A., & Lees, E. (1998). Active cdk6 complexes are predominantly nuclear and represent only a minority of the cdk6 in T cells. Oncogene, 16(5), 603-611. doi: 10.1038/sj.onc.1201570 PMID: 9482106

Malladi, S., Challa-Malladi, M., Fearnhead, H. O., & Bratton, S. B. (2009). The Apaf-1*procaspase-9 apoptosome complex functions as a proteolytic-based molecular timer. EMBO J, 28(13), 1916-1925. doi: 10.1038/emboj.2009.152 PMID: 19494828

Malumbres, M., & Barbacid, M. (2001). To cycle or not to cycle: a critical decision in cancer. Nat Rev Cancer, 1(3), 222-231. doi: 10.1038/35106065 PMID: 11902577

Manning, B. D., & Toker, A. (2017). AKT/PKB Signaling: Navigating the Network. Cell, 169(3), 381-405. doi: 10.1016/j.cell.2017.04.001 PMID: 28431241

Markou, A., Tsaroucha, E. G., Kaklamanis, L., Fotinou, M., Georgoulias, V., & Lianidou, E. S. (2008). Prognostic value of mature microRNA-21 and microRNA-205 overexpression in non-small cell lung cancer by quantitative real-time RT-PCR. Clin Chem, 54(10), 1696-1704. doi: 10.1373/clinchem.2007.101741 PMID: 18719201

Marzec, M., Kasprzycka, M., Lai, R., Gladden, A. B., Wlodarski, P., Tomczak, E., . . . Wasik, M. A. (2006). Mantle cell lymphoma cells express predominantly cyclin D1a isoform and are highly sensitive to selective inhibition of CDK4 kinase activity. Blood, 108(5), 1744-1750. doi: 10.1182/blood-2006-04-016634 PMID: 16690963

Mayr, C., Hemann, M. T., & Bartel, D. P. (2007). Disrupting the pairing between let-7 and Hmga2 enhances oncogenic transformation. Science, 315(5818), 1576-1579. doi: 10.1126/science.1137999 PMID: 17322030

McMahon C., Tuangporn S., Di Renzo J., Ewen M.E. P/CAF associates with cyclin D1 and potentiates its activation of the estrogen receptor. Proc. Natl. Acad. Sci. USA. 1999;96:5382–5387. doi: 10.1073/pnas.96.10.5382.

Micheva, K. D., Vallee, A., Beaulieu, C., Herman, I. M., & Leclerc, N. (1998). beta-Actin is confined to structures having high capacity of remodelling in developing and adult rat cerebellum. Eur J Neurosci, 10(12), 3785-3798. doi: 10.1046/j.1460-9568.1998.00391.x PMID: 9875357

Monaco, G., Decrock, E., Arbel, N., van Vliet, A. R., La Rovere, R. M., De Smedt, H., . . . Bultynck, G. (2015). The BH4 domain of anti-apoptotic Bcl-XL, but not that of the related Bcl-2, limits the voltage-dependent anion channel 1 (VDAC1)-mediated transfer of pro-apoptotic Ca2+ signals to mitochondria. J Biol Chem, 290(14), 9150-9161. doi: 10.1074/jbc.M114.622514 PMID: 25681439

Morgan, D. O. (1997). Cyclin-dependent kinases: engines, clocks, and microprocessors. Annu Rev Cell Dev Biol, 13, 261-291. doi: 10.1146/annurev.cellbio.13.1.261 PMID: 9442875

Mori, R., Wang, Q., Danenberg, K. D., Pinski, J. K., & Danenberg, P. V. (2008). Both beta-actin and GAPDH are useful reference genes for normalization of quantitative RT-PCR in human FFPE tissue samples of prostate cancer. Prostate, 68(14), 1555-1560. doi: 10.1002/pros.20815 PMID: 18651557

Muchmore, S. W., Sattler, M., Liang, H., Meadows, R. P., Harlan, J. E., Yoon, H. S., . . . Fesik, S. W. (1996). X-ray and NMR structure of human Bcl-xL, an inhibitor of programmed cell death. Nature, 381(6580), 335-341. doi: 10.1038/381335a0 PMID: 8692274

Mueller, T., Voigt, W., Simon, H., Fruehauf, A., Bulankin, A., Grothey, A., & Schmoll, H. J. (2003). Failure of activation of caspase-9 induces a higher threshold for apoptosis and cisplatin resistance in testicular cancer. Cancer Res, 63(2), 513-521. PMID: 12543810

Mundi, P. S., Sachdev, J., McCourt, C., & Kalinsky, K. (2016). AKT in cancer: new molecular insights and advances in drug development. Br J Clin Pharmacol, 82(4), 943-956. doi: 10.1111/bcp.13021 PMID: 27232857

Munster P, et al. Abstract P4-22-18: phase Ib safety, efficacy, and molecular analysis of ribociclib (LEE011) plus letrozole for the treatment of ER+, HER2– advanced breast cancer. Cancer Res 2017; 77: P4–22-18–P4-22-18.

Murakami, Y., Yasuda, T., Saigo, K., Urashima, T., Toyoda, H., Okanoue, T., & Shimotohno, K. (2006). Comprehensive analysis of microRNA expression patterns in hepatocellular carcinoma and non-tumorous tissues. Oncogene, 25(17), 2537-2545. doi: 10.1038/sj.onc.1209283 PMID: 16331254

Musgrove, E. A., Caldon, C. E., Barraclough, J., Stone, A., & Sutherland, R. L. (2011). Cyclin D as a therapeutic target in cancer. Nat Rev Cancer, 11(8), 558-572. doi: 10.1038/nrc3090 PMID: 21734724

Nowak, D., Krawczenko, A., Dus, D., & Malicka-Blaszkiewicz, M. (2002). Actin in human colon adenocarcinoma cells with different metastatic potential. Acta Biochim Pol, 49(4), 823-828. PMID: 12545189

Nowak, D., Skwarek-Maruszewska, A., Zemanek-Zboch, M., & Malicka-Blaszkiewicz, M. (2005). Beta-actin in human colon adenocarcinoma cell lines with different metastatic potential. Acta Biochim Pol, 52(2), 461-468. PMID: 15940343

O'Brien NA, Tomaso ED, Ayala R, et al. In vivo efficacy of combined targeting of CDK4/6, ER and PI3K signaling in ER+ breast cancer. Cancer Res 2014; 74:19 Suppl:4756-4756. abstract.

Ohl, F., Jung, M., Xu, C., Stephan, C., Rabien, A., Burkhardt, M., . . . Jung, K. (2005). Gene expression studies in prostate cancer tissue: which reference gene should be selected for normalization? J Mol Med (Berl), 83(12), 1014-1024. doi: 10.1007/s00109-005-0703-z PMID: 16211407

Okamura, K., Hagen, J. W., Duan, H., Tyler, D. M., & Lai, E. C. (2007). The mirtron pathway generates microRNA-class regulatory RNAs in Drosophila. Cell, 130(1), 89-100. doi: 10.1016/j.cell.2007.06.028 PMID: 17599402

Okamura, K., Liu, N., & Lai, E. C. (2009). Distinct mechanisms for microRNA strand selection by Drosophila Argonautes. Mol Cell, 36(3), 431-444. doi: 10.1016/j.molcel.2009.09.027 PMID: 19917251

Oudejans, J. J., Muris, J. J., & Meijer, C. J. (2005). Inhibition of caspase 9 and not caspase 8 mediated apoptosis may determine clinical response to chemotherapy in primary nodal diffuse large B-cell lymphomas. Cell Cycle, 4(4), 526-528. doi: 10.4161/cc.4.4.1595 PMID: 15876872

Park, J. Y., Park, J. M., Jang, J. S., Choi, J. E., Kim, K. M., Cha, S. I., . . . Jung, T. H. (2006). Caspase 9 promoter polymorphisms and risk of primary lung cancer. Hum Mol Genet, 15(12), 1963-1971. doi: 10.1093/hmg/ddl119 PMID: 16687442

Patnaik, A., Rosen, L. S., Tolaney, S. M., Tolcher, A. W., Goldman, J. W., Gandhi, L., . . . Shapiro, G. I. (2016). Efficacy and Safety of Abemaciclib, an Inhibitor of CDK4 and CDK6, for Patients with Breast Cancer, Non-Small Cell Lung Cancer, and Other Solid Tumors. Cancer Discov, 6(7), 740-753. doi: 10.1158/2159-8290.CD-16-0095 PMID: 27217383

Pollard, T. D., & Borisy, G. G. (2003). Cellular motility driven by assembly and disassembly of actin filaments. Cell, 112(4), 453-465. doi: 10.1016/s0092-8674(03)00120-x PMID: 12600310

Polyak, K., Lee, M. H., Erdjument-Bromage, H., Koff, A., Roberts, J. M., Tempst, P., & Massague, J. (1994). Cloning of p27Kip1, a cyclin-dependent kinase inhibitor and

a potential mediator of extracellular antimitogenic signals. Cell, 78(1), 59-66. doi: 10.1016/0092-8674(94)90572-x PMID: 8033212

Popow, A., Nowak, D., & Malicka-Blaszkiewicz, M. (2006). Actin cytoskeleton and beta-actin expression in correlation with higher invasiveness of selected hepatoma Morris 5123 cells. J Physiol Pharmacol, 57 Suppl 7, 111-123. PMID: 17228099

Pfizer: Ibrance package insert. http://labeling.pfizer.com/ShowLabeling.aspx?id=2191

Qian, B., Katsaros, D., Lu, L., Preti, M., Durando, A., Arisio, R., . . . Yu, H. (2009). High miR-21 expression in breast cancer associated with poor disease-free survival in early stage disease and high TGF-beta1. Breast Cancer Res Treat, 117(1), 131-140. doi: 10.1007/s10549-008-0219-7 PMID: 18932017

Qin, H., Srinivasula, S. M., Wu, G., Fernandes-Alnemri, T., Alnemri, E. S., & Shi, Y. (1999). Structural basis of procaspase-9 recruitment by the apoptotic protease-activating factor 1. Nature, 399(6736), 549-557. doi: 10.1038/21124 PMID: 10376594

Reutens, A. T., Fu, M., Wang, C., Albanese, C., McPhaul, M. J., Sun, Z., . . . Pestell, R. G. (2001). Cyclin D1 binds the androgen receptor and regulates hormone-dependent signaling in a p300/CBP-associated factor (P/CAF)-dependent manner. Mol Endocrinol, 15(5), 797-811. doi: 10.1210/mend.15.5.0641 PMID: 11328859

Rodriguez A, Griffiths-Jones S, Ashurst JL, et al. Identification of mammalian microRNA host genes and transcription units. Genome Res. 2004; 14:1902–1910. [PubMed: 15364901]

Ruan, W., & Lai, M. (2007). Actin, a reliable marker of internal control? Clin Chim Acta, 385(1-2), 1-5. doi: 10.1016/j.cca.2007.07.003 PMID: 17698053

Saini, H. K., Griffiths-Jones, S., & Enright, A. J. (2007). Genomic analysis of human microRNA transcripts. Proc Natl Acad Sci U S A, 104(45), 17719-17724. doi: 10.1073/pnas.0703890104 PMID: 17965236

Sampson, V. B., Rong, N. H., Han, J., Yang, Q., Aris, V., Soteropoulos, P., . . . Krueger, L. J. (2007). MicroRNA let-7a down-regulates MYC and reverts MYC-induced growth in Burkitt lymphoma cells. Cancer Res, 67(20), 9762-9770. doi: 10.1158/0008-5472.CAN-07-2462 PMID: 17942906

Sanchez-Martinez, C., Gelbert, L. M., Lallena, M. J., & de Dios, A. (2015). Cyclin dependent kinase (CDK) inhibitors as anticancer drugs. Bioorg Med Chem Lett, 25(17), 3420-3435. doi: 10.1016/j.bmcl.2015.05.100 PMID: 26115571

Saraiya, A. A., & Wang, C. C. (2008). snoRNA, a novel precursor of microRNA in Giardia lamblia. PLoS Pathog, 4(11), e1000224. doi: 10.1371/journal.ppat.1000224 PMID: 19043559

Schwarz, D. S., Hutvagner, G., Du, T., Xu, Z., Aronin, N., & Zamore, P. D. (2003). Asymmetry in the assembly of the RNAi enzyme complex. Cell, 115(2), 199-208. doi: 10.1016/s0092-8674(03)00759-1 PMID: 14567917

Shi, Y., Liu, X., Han, E. K., Guan, R., Shoemaker, A. R., Oleksijew, A., . . . Luo, Y. (2005). Optimal classes of chemotherapeutic agents sensitized by specific small-molecule inhibitors of akt in vitro and in vivo. Neoplasia, 7(11), 992-1000. doi: 10.1593/neo.05355 PMID: 16331885

Singh, M., & Johnson, L. (2006). Using genetically engineered mouse models of cancer to aid drug development: an industry perspective. Clin Cancer Res, 12(18), 5312-5328. doi: 10.1158/1078-0432.CCR-06-0437 PMID: 17000664

Soos, T. J., Kiyokawa, H., Yan, J. S., Rubin, M. S., Giordano, A., DeBlasio, A., . . . Koff, A. (1996). Formation of p27-CDK complexes during the human mitotic cell cycle. Cell Growth Differ, 7(2), 135-146. PMID: 8822197

Spring, L. M., Zangardi, M. L., Moy, B., & Bardia, A. (2017). Clinical Management of Potential Toxicities and Drug Interactions Related to Cyclin-Dependent Kinase 4/6 Inhibitors in Breast Cancer: Practical Considerations and Recommendations. Oncologist, 22(9), 1039-1048. doi: 10.1634/theoncologist.2017-0142 PMID: 28706010

Sugimoto, M., Martin, N., Wilks, D. P., Tamai, K., Huot, T. J., Pantoja, C., . . . Hara, E. (2002). Activation of cyclin D1-kinase in murine fibroblasts lacking both p21(Cip1) and p27(Kip1). Oncogene, 21(53), 8067-8074. doi: 10.1038/sj.onc.1206019 PMID: 12444543

Takaki, T., Echalier, A., Brown, N. R., Hunt, T., Endicott, J. A., & Noble, M. E. (2009). The structure of CDK4/cyclin D3 has implications for models of CDK activation. Proc Natl Acad Sci U S A, 106(11), 4171-4176. doi: 10.1073/pnas.0809674106 PMID: 19237555

Theodoropoulos, G. E., Gazouli, M., Vaiopoulou, A., Leandrou, M., Nikouli, S., Vassou, E., . . . Nikiteas, N. (2011). Polymorphisms of caspase 8 and caspase 9 gene and colorectal cancer susceptibility and prognosis. Int J Colorectal Dis, 26(9), 1113-1118. doi: 10.1007/s00384-011-1217-5 PMID: 21538054

Theodoropoulos, G. E., Michalopoulos, N. V., Panoussopoulos, S. G., Taka, S., & Gazouli, M. (2010). Effects of caspase-9 and survivin gene polymorphisms in pancreatic cancer risk and tumor characteristics. Pancreas, 39(7), 976-980. doi:

Tsujimoto, Y., & Croce, C. M. (1986). Analysis of the structure, transcripts, and protein products of bcl-2, the gene involved in human follicular lymphoma. Proc Natl Acad Sci U S A, 83(14), 5214-5218. doi: 10.1073/pnas.83.14.5214 PMID: 3523487

Tsujimoto, Y., Finger, L. R., Yunis, J., Nowell, P. C., & Croce, C. M. (1984). Cloning of the chromosome breakpoint of neoplastic B cells with the t(14;18) chromosome translocation. Science, 226(4678), 1097-1099. doi: 10.1126/science.6093263 PMID: 6093263

Tolaney SM, et al. Ribociclib + fulvestrant in postmenopausal women with HR+, HER2– advanced breast cancer (ABC). In: San Antonio Breast Cancer Symposium, 6–10 December 2016, Springer Healthcare Limited: San Antonio, Texas. pp.1027–1028.

Toogood, P. L., Harvey, P. J., Repine, J. T., Sheehan, D. J., VanderWel, S. N., Zhou, H., . . . Fry, D. W. (2005). Discovery of a potent and selective inhibitor of cyclin-dependent kinase 4/6. J Med Chem, 48(7), 2388-2406. doi: 10.1021/jm049354h PMID: 15801831

Toyoshima, H., & Hunter, T. (1994). p27, a novel inhibitor of G1 cyclin-Cdk protein kinase activity, is related to p21. Cell, 78(1), 67-74. doi: 10.1016/0092-8674(94)90573-8 PMID: 8033213

Trang, P., Wiggins, J. F., Daige, C. L., Cho, C., Omotola, M., Brown, D., . . . Slack, F. J. (2011). Systemic delivery of tumor suppressor microRNA mimics using a neutral lipid emulsion inhibits lung tumors in mice. Mol Ther, 19(6), 1116-1122. doi: 10.1038/mt.2011.48 PMID: 21427705

Tripathy, D., Bardia, A., & Sellers, W. R. (2017). Ribociclib (LEE011): Mechanism of Action and Clinical Impact of This Selective Cyclin-Dependent Kinase 4/6 Inhibitor in Various Solid Tumors. Clin Cancer Res, 23(13), 3251-3262. doi: 10.1158/1078-0432.CCR-16-3157 PMID: 28351928

Vervliet, T., Lemmens, I., Vandermarliere, E., Decrock, E., Ivanova, H., Monaco, G., . . . Bultynck, G. (2015). Ryanodine receptors are targeted by anti-apoptotic Bcl-XL involving its BH4 domain and Lys87 from its BH3 domain. Sci Rep, 5, 9641. doi: 10.1038/srep09641 PMID: 25872771

Verzenio [package insert]. Indianapolis, IN: Lilly USA, LLC; 2018.

Visone, R., Pallante, P., Vecchione, A., Cirombella, R., Ferracin, M., Ferraro, A., . . . Fusco, A. (2007). Specific microRNAs are downregulated in human thyroid anaplastic carcinomas. Oncogene, 26(54), 7590-7595. doi: 10.1038/sj.onc.1210564 PMID: 17563749

Volinia, S., Calin, G. A., Liu, C. G., Ambs, S., Cimmino, A., Petrocca, F., . . . Croce, C. M. (2006). A microRNA expression signature of human solid tumors defines cancer gene targets. Proc Natl Acad Sci U S A, 103(7), 2257-2261. doi: 10.1073/pnas.0510565103 PMID: 16461460

Walker, J. C., & Harland, R. M. (2009). microRNA-24a is required to repress apoptosis in the developing neural retina. Genes Dev, 23(9), 1046-1051. doi: 10.1101/gad.1777709 PMID: 19372388

Wang, J., Zhao, W., Guo, H., Fang, Y., Stockman, S. E., Bai, S., . . . Ding, Z. (2018). AKT isoform-specific expression and activation across cancer lineages. BMC Cancer, 18(1), 742. doi: 10.1186/s12885-018-4654-5 PMID: 30012111

Waxman, S., & Wurmbach, E. (2007). De-regulation of common housekeeping genes in hepatocellular carcinoma. BMC Genomics, 8, 243. doi: 10.1186/1471-2164-8-243 PMID: 17640361

Wightman, B., Ha, I., & Ruvkun, G. (1993). Posttranscriptional regulation of the heterochronic gene lin-14 by lin-4 mediates temporal pattern formation in C. elegans. Cell, 75(5), 855-862. doi: 10.1016/0092-8674(93)90530-4 PMID: 8252622

Wu, G. S., & Ding, Z. (2002). Caspase 9 is required for p53-dependent apoptosis and chemosensitivity in a human ovarian cancer cell line. Oncogene, 21(1), 1-8. doi: 10.1038/sj.onc.1205020 PMID: 11791171

Wu, H., Xu, H., Miraglia, L. J., & Crooke, S. T. (2000). Human RNase III is a 160-kDa protein involved in preribosomal RNA processing. J Biol Chem, 275(47), 36957-36965. doi: 10.1074/jbc.M005494200 PMID: 10948199

Yan, L. X., Huang, X. F., Shao, Q., Huang, M. Y., Deng, L., Wu, Q. L., . . . Shao, J. Y. (2008). MicroRNA miR-21 overexpression in human breast cancer is associated with advanced clinical stage, lymph node metastasis and patient poor prognosis. RNA, 14(11), 2348-2360. doi: 10.1261/rna.1034808 PMID: 18812439

Yanaihara, N., Caplen, N., Bowman, E., Seike, M., Kumamoto, K., Yi, M., . . . Harris, C. C. (2006). Unique microRNA molecular profiles in lung cancer diagnosis and prognosis. Cancer Cell, 9(3), 189-198. doi: 10.1016/j.ccr.2006.01.025 PMID: 16530703

Yang, C., Li, Z., Bhatt, T., Dickler, M., Giri, D., Scaltriti, M., . . . Chandarlapaty, S. (2017). Acquired CDK6 amplification promotes breast cancer resistance to

CDK4/6 inhibitors and loss of ER signaling and dependence. Oncogene, 36(16), 2255-2264. doi: 10.1038/onc.2016.379 PMID: 27748766

Yi, R., Qin, Y., Macara, I. G., & Cullen, B. R. (2003). Exportin-5 mediates the nuclear export of pre-microRNAs and short hairpin RNAs. Genes Dev, 17(24), 3011-3016. doi: 10.1101/gad.1158803 PMID: 14681208

Yu, F., Yao, H., Zhu, P., Zhang, X., Pan, Q., Gong, C., . . . Song, E. (2007). let-7 regulates self renewal and tumorigenicity of breast cancer cells. Cell, 131(6), 1109-1123. doi: 10.1016/j.cell.2007.10.054 PMID: 18083101

Zelivianski, S., Cooley, A., Kall, R., & Jeruss, J. S. (2010). Cyclin-dependent kinase 4-mediated phosphorylation inhibits Smad3 activity in cyclin D-overexpressing breast cancer cells. Mol Cancer Res, 8(10), 1375-1387. doi: 10.1158/1541-7786.MCR-09-0537 PMID: 20736297

Zhou, G. L., Tucker, D. F., Bae, S. S., Bhatheja, K., Birnbaum, M. J., & Field, J. (2006). Opposing roles for Akt1 and Akt2 in Rac/Pak signaling and cell migration. J Biol Chem, 281(47), 36443-36453. doi: 10.1074/jbc.M600788200 PMID: 17012749

.